ELSEVIER ELSEVIER

Contents lists available at ScienceDirect

Dendrochronologia

journal homepage: www.elsevier.com/locate/dendro





Recent growth increase in endemic *Juglans boliviana* from the tropical Andes

Rose C. Oelkers ^{a,b,*}, Laia Andreu-Hayles ^{a,c,d}, Rosanne D'Arrigo ^a, Arturo Pacheco-Solana ^a, Milagros Rodriguez-Caton ^{a,e}, Alfredo Fuentes ^{f,g}, Guaciara M. Santos ^h, Ernesto Tejedor ⁱ, M. Eugenia Ferrero ^j, Carla Maldonado ^f

- ^a Tree-ring Laboratory, Lamont-Doherty Earth Observatory of Columbia University, Palisades, NY 10964, USA
- ^b Department of Earth and Environmental Science, Columbia University, New York, NY 10027, USA
- ^c CREAF, Bellaterra, Barcelona, Spain
- d ICREA, Pg. Lluís Companys, 23, Barcelona, Spain
- ^e Department of Plant Sciences, University of California Davis, CA 95616, USA
- f Herbario Nacional de Bolivia. Instituto de Ecología. Universidad Mayor de San Andrés. La Paz. Bolivia
- g Center for Conservation and Sustainable Development, Missouri Botanical Garden, St. Louis, MO, USA
- ^h Earth System Science Department, University of California, B321 Croul Hall, Irvine, CA 92697-3100, USA
- ¹ Department of Geology, National Museum of Natural Sciences (MNCN), CSIC, Madrid, Spain
- ^j Instituto Argentino de Nivología, Glaciología y Ciencias Ambientales (IANIGLA), CONICET-Universidad Nacional de Cuyo, CP5500, CC330, Mendoza, Argentina

ARTICLE INFO

Keywords: Amazon-Andes transition forest Wood anatomy Tree rings Radiocarbon Tropical dendrochronology Bolivian Yungas

ABSTRACT

The spatial coverage of tree-ring chronologies in tropical South America is low compared to the extratropics, particularly in remote regions. Tree-ring dating from such tropical sites is limited by the generally weak temperature seasonality, complex coloration, and indistinct anatomical morphology in some tree species. As a result, there is a need to complement traditional methods of dendrochronology with innovative and independent approaches. Here, we supplement traditional tree-ring methods via the use of radiocarbon analyses to detect partial missing rings and/or false rings, and wood anatomical techniques to precisely delineate tree-ring boundaries. In so doing we present and confirm the annual periodicity of the first tree-ring width (TRW) chronology spanning from 1814 to 2017 for Juglans boliviana ('nogal'), a tree species growing in a mid-elevation tropical moist forest in northern Bolivia. We collected 25 core samples and 4 cross-sections from living and recently harvested canopy-dominant trees, respectively. The sampled trees were growing in the Madidi National Park and had a mean age of 115 years old, with certain trees growing for over 200 years. Comparison of (residual and standard) TRW chronologies to monthly climate variables shows significant negative relationships to prior year May-August maximum temperatures (r = -0.54, p < 0.05) and positive relationships to dry season May-October precipitation (r = 0.60, p < 0.05) before the current year growing season. Additionally, the radial growth of Juglans boliviana shows a significant positive trend since 1979. Our findings describe a new and promising tree species for dendrochronology due to its longevity and highlight interdisciplinary techniques that can be used to expand the current tree-ring network in Bolivia and the greater South American tropics.

1. Introduction

The tropical Andes of South America (~10°N-24°S) is one of the Earth's greatest hotspots for biodiversity, yet among the least explored settings for dendrochronology (Quesada-Román et al., 2022; Schöngart et al., 2017). Tree-ring analysis in the diverse mid-lowland forests of the Andes can be extremely challenging, due to the lack of annual

periodicity of growth layers and/or well-defined tree-ring boundaries in many tree species, leading to difficulties in cross dating (i.e. finding agreement in growth patterns among trees). Further, there is only a limited understanding of the factors contributing to tropical tree growth and dormancy in the tropical Andes and other low latitude locations (Boninsegna et al., 2009; Morales et al., 2020; Zuidema et al., 2022). Early studies in tropical dendrochronology suggested that tree species

^{*} Corresponding author at: Tree-ring Laboratory, Lamont-Doherty Earth Observatory of Columbia University, Palisades, NY 10964, USA. E-mail address: roelkers@ldeo.columbia.edu (R.C. Oelkers).

that endure dry periods for more than two months could trigger cambial dormancy and form distinguishable ring boundaries (Worbes, 1999), but cambial dormancy can also occur for both endogenous (i.e. sub-annual physiological defoliation (Brienen et al., 2016), competition for sunlight (Carlquist, 2001)), or exogenous reasons (i.e.; solar radiation, frost; Fritts, 1976). For tree species in extremely humid forests with high seasonal precipitation variability (like the Bolivian Yungas study here), the coherency in growth patterns within and between trees can be very low. Due to the complexity of tropical wood anatomy and the minimal agreement among trees in some species and settings, supplementary dating methods, such as radiocarbon analyses (14C), have been used to independently confirm dendrochronological results (Baker et al., 2017; Herrera-Ramirez et al., 2017; Pacheco-Solana et al., 2023). Radiocarbon and traditional dendrochronological processing (i.e., crossdating) are thus complementary, yet time-consuming, baselines for tree-ring chronology development in many settings in the tropics and both methods will be used herein.

In recent decades there has been much promise in the development of tree-ring chronologies in the tropical Andes. This is particularly true for the region of the vast Altiplano $(15^{\circ}-22^{\circ}S)$ the highest (~4000 m a. s.l.) and most expansive (~1000 km) plateau of the Andes, that spans the entirety of western Bolivia, where climate-sensitive Polylepis tarapacana trees older than 700 years have been found (Morales et al., 2012). A number of these tree-ring chronologies have recorded regional precipitation for the last centuries as well as inter-annual variability related to El Niño-Southern Oscillation (ENSO), a global scale atmosphere-ocean phenomenon related to Pacific Ocean sea-surface temperatures anomalies (SSTA's) that profoundly influences the hydroclimate of South America and the globe (Morales et al., 2020). Most existing tree-ring chronologies in eastern Bolivia are from low elevation (< 500 m a.s.l.) dry forests and feature Anacardiaceae species like Schinopsis brasiliensis (López and Villalba, 2016) and members of the Fabaceae family such as Amburana cearensis (López et al., 2022; Paredes-Villanueva et al., 2015), Machaerium scleroxylon (Paredes-Villanueva et al., 2013), and Centrolobium microchaete (López and Villalba, 2011), while humid submontane ecosystems (1100-1800 m a.s.l.) remain largely unsampled.

Although the number of published, well-dated tree-ring chronologies in the Bolivian Amazon is still quite low, there has been considerable progress over the past 1–2 decades in identifying tree species (mostly semi-deciduous and from the Fabaceae and Moraceae families) useful for dendrochronology which can grow in moist forests and form annual rings: e.g. Clarisia racemosa (Soliz-Gamboa et al., 2011), Ampelocera ruizii, Albizia niopioides, Cariniana ianeirensis, Centrolobium microchaete, Ficus boliviana (evergreen), Hura crepitans, Pseudolmedia laevis (López et al., 2012), Amburana cearensis, Bertholletia excelsa (evergreen), Cedrelinga catenaeformis, Cedrela odorata, Tachigali vasquezii, Peltogyne heterophylla (Brienen, 2005; Brienen and Zuidema, 2006). Pioneering tree-ring research in Bolivia's Madidi National Park (MNP) reported a deciduous Pseudolmedia rigida tree with annual periodicity and thus, potential for tree-ring studies (Andreu-Hayles et al., 2015).

Here we describe the first documented tree-ring width (TRW) chronology for *Juglans boliviana* growing in the MNP. *Juglans boliviana* ([C. DC. Dode 1909]), commonly referred to as "nogal", or "nogal boliviano", is a tropical walnut endemic to the submontane moist environments of Southern Peru (> 8°S) and Northern Bolivia (< 19°S) (Fuentes, 2005; La Porte, 1966; Manning, 1960; Miller, 1976; Stone et al., 2009). As it is the case for other *Juglandaceae* in South America, the wood is used for both economic (e.g. timber, dye) and medicinal purposes (e.g. kidney disease) particularly within indigenous communities (Araujo-Murakami et al., 2006; De Lucca and Zalles, 1992; Paniagua-Zambrana et al., 2020). Despite its socioeconomic and environmental value, little is known about the growth cycle and longevity of these shade intolerant angiosperms (Mostacedo C and Fredericksen, 1999).

Several species of *Juglans* trees from tropical South America have been used in dendrochronological studies, including *Juglans australis* (Ferrero et al., 2015, 2013; Morales et al., 2004; Villalba et al., 1985)

and *Juglans neotropica* (Humanes-Fuente et al., 2020; Inga and del Valle, 2017). The biggest difference among these tropical black walnuts species resides in the leaf and fruit physiology (Manning, 1960, 1948), whereas their diffuse porous wood anatomy looks largely the same (Miller, 1976). *Juglans australis* represents the southernmost neotropical specimen of the genus, ranging from ~20°S to 27°S, while *Juglans neotropica* is more widespread in the North-Central Andes spanning from ~9°S to 14°S (Stone et al., 2009; Manning, 1960). Dendrochronological studies have confirmed that South American *Juglans* can be quite long-lived (> 300 years), are in both tropical (Peru and Bolivia) and subtropical (Argentina) montane environments and feature annual tree growth variability that is positively correlated with precipitation (Humanes-Fuente et al., 2020; Villalba et al., 1998). However, to our knowledge, *Juglans boliviana* has not yet been evaluated for this purpose.

Here we study a new *Juglans* species for dendrochronology endemic to the Bolivian and Peruvian Yungas. First, we confirm the annual periodicity of *Juglans boliviana* using both traditional dendrochronology and radiocarbon analysis, as well as wood anatomical techniques, to produce a robust tree-ring width chronology. Second, we use this new record to assess the growth variability and trends and climate sensitivity at this site to report the dendrochronological potential of long-lived *Juglans boliviana* growing in primary forests of tropical Bolivia.

2. Materials and methods

2.1. Site description and climatology

One of the most extensive protected areas in Bolivia is the MNP, located in the northwestern corner of the country. Its complex topography supports a range of forest types, from dry subhumid montane to lowland wet environments that feature diverse primary stands and fragile, threatened tree species (Araujo-Murakami et al., 2006; Fuentes, 2005; Macía, 2008). The MNP corridor serves as a transitional zone between the Amazon basin and the Andes. Due to its distinct seasonality, preserved old growth forests, pronounced elevational gradient, and high diversity, it holds great promise for expanding tropical South American tree-ring research.

Our study site is in a seasonally humid Amazon-Andes transitional forest (~1300 m a.s.l.) on a north facing slope near the town of Santa Rosa in the MNP (14.40°S, 68.42°W) (Fig. 1 A). The landscape is characterized by closed-canopy forests and seems to be an old growth area that has remained relatively undisturbed. However, there are signs of mining and small-scale farming along the river banks of the Rio Tuichi (1000 m a.s.l.), which is a tributary of the Madeira River basin ~2 km away from our sampling site. Juglans boliviana dominates the canopy of this diverse semi-evergreen forest along with the presence of a rare palm Dictyocaryum lamarckianum, which is an indicator species for the low-tomid elevation submontane environment (Fig. 1 A,C) (Fuentes, 2005). The forest interior features thick layers of herbaceous understory, subcanopy, and few lianas growing upon a moist layer of leaf litter and well-drained sandy clay soils. Accompanying woody species included a mix of mature evergreen (Erisma uncinatum, Astronium graveolons) and deciduous trees (Cedrela fissilis, Pseudolmedia laevis, Platymiscium pinnatum).

This area receives 1345 mm of rain on average per year, mainly from October through May, and has a short dry season from June/July to August (Fig. 1B). Temperatures range between 10.5 °C (minimum, July) and 24 °C (maximum, November) with a mean annual temperature of 17.5 °C. The phenology of *Juglans boliviana* is poorly understood, though studies of *Juglans neotropica* growing in similar Andean environments suggest leaf-out (i.e. foliation of new leaves) initiates during the onset of the wet season and partial (or complete) defoliation occurs during the dry season as temperatures cool and fruits mature (Ramírez and Kallarackal, 2021; Vanegas and Rojas, 2018). At the time of sampling in July, the *Juglans boliviana* trees appeared to have partially intact leaves and developed fruits. Based on the mean climatology for this site

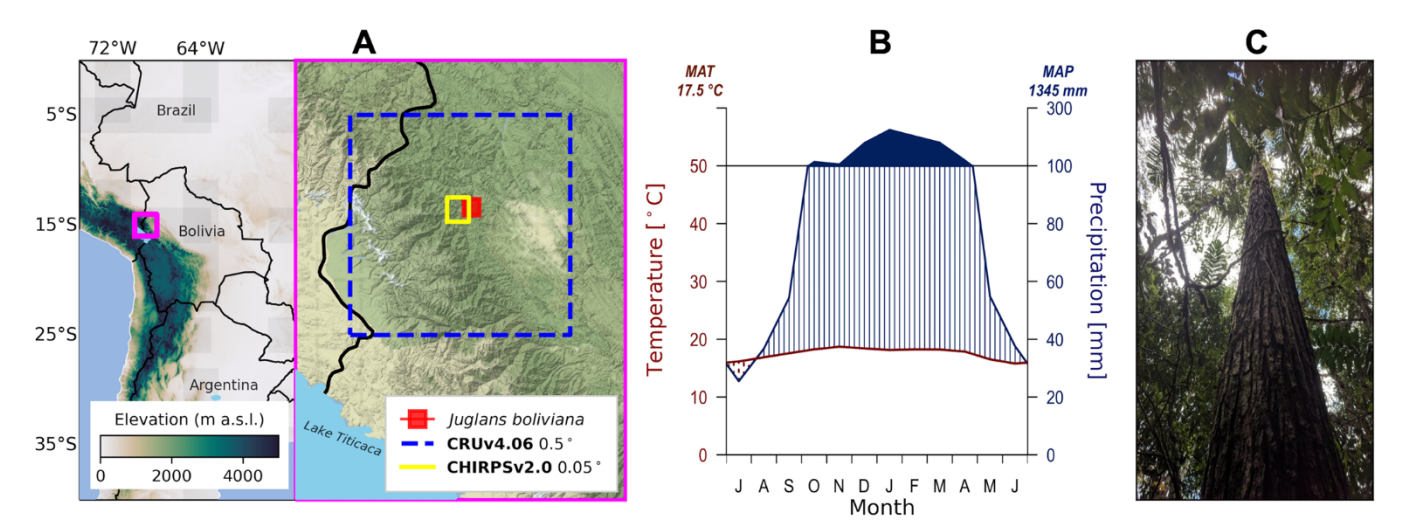


Fig. 1. (A) Location and elevation of *Juglans boliviana* site (red square) plotted with the nearest CHIRPS 2.0 (0.05°, yellow) and CRU 4.06 (0.5°, blue) grids used in climate analysis in northwestern Bolivia. (B) The mean climatology (1981–2018) based on the CRU gridpoint shows this site endures a long wet-period between October-May (austral spring and summer) and short, dry, winter season (June-July). (C) Photo of one of the *J. boliviana* trees cored in July 2018. Most individual trees reached the canopy in this moist mid-elevation site.

(Fig. 1B) and phenotypic studies of other tropical *Juglans* in the vicinity of the Andes, we assume that the growing season for the *Juglans boliviana* in this location likely occurs sometime between October-May.

2.2. Sample collection and dendrochronological processing

In 2018, we sampled 29 individual trees of Juglans boliviana, near an ecological plot maintained by the National Herbarium of Bolivia. Our sampling campaign was conducted in collaboration with field botanists from the National Herbarium of Bolivia, who facilitated botanical identification of tree species, along with members of the local community of Santa Rosa. The voucher herbarium specimen 4113 A (LPB) from Cayola et al. represents a botanical sample of Juglans bolviana collected from a nearby plot in the year 2010 which can be accessed online via the specimen database Tropicos TM (https://www.tropicos.org/specimen/ Search). The average diameter of the trees sampled in this study was 74 cm at breast height, with some trees growing as large as 137 cm in diameter. Using a nondestructive, 2-threaded (minimum 16 in.) increment borer, 3-4 core samples were extracted from 25 living trees at 1.2 m above ground. Although this is a hardwood species, coring the wood (which was saturated with water), was simple (wood density 0.55–0.7 g/cm³). Additionally, whole slabs of wood from recently harvested trees near the forest perimeter were cut using a chainsaw. Local community members noted that these trees may have been felled between 2015 and 2018. All the samples were shipped to the Tree-Ring Laboratory of the Lamont-Doherty Earth Observatory (LDEO) in the Palisades (NY, USA), where they were carefully sanded using a variety of grits with both orbital sanders and manually with microfiber paper.

2.3. Crossdating and measuring tree-ring width at MNP

Once the samples were sanded, we used a combination of two crossdating techniques. The list method (Yamaguchi, 1991) entails the manual recording and visual comparison of distinct features of rings (e. g. narrow, wide, less latewood, etc.) under a stereomicroscope. Under the stereomicroscope, non-LED light bulbs (such as yellow or red) were used to improve visualization of the dark purple wood samples characteristic of Bolivian walnut trees. A total of 16 cores and 4 cross sections were dated (based on the list method) and scanned with a white background (due to the dark complexion of the wood) using an Epson Expression 1100000XL at 3200 dpi. The second crossdating technique involved the use of the image analysis software CooRecorder with

Cdendro (Cybis Elektronik & Data AB, 2022; http://www.cybis.se/for-fun/dendro/helpcoorecorder7/index.htm) to visually compare the growth patterns among and within individual trees samples from the site.

The dating process for Juglans tree rings is time consuming and labor intensive due to the complex anatomy and irregular nature of the wood. The designated year of field collection provides an initial starting calendar date for the most recent ring boundary in the living samples. For example, for samples collected in July 2018, the first full ring behind the bark represents the growing season that began in austral spring 2017 and ended in austral summer 2018. Based on the Shulman convention (Schulman, 1956), this ring is assigned to the year that the tree starts growing (2017), assuming that part of the growth also takes place in the year 2018. Each ring is thereafter assigned a date back in time until the pith, or the earliest formed ring available in the sample, is reached. Once dates were assigned to the rings, the width of each year across all samples (depicted as 0.001 mm) was measured digitally in CooRecorder (Cybis Elektronik & Data AB) for a total of 45 series. To further check the quality of our crossdating and ring-width measurements, we used computer assisted programs such as Cofecha (Holmes, 1983) and Cdendro (http://www.cybis.se/forfun/dendro/).

2.4. Radiocarbon analyses

To independently verify our initial visual and statistically cross-dating, radiocarbon (14 C) content was measured from the cellulose of individual tree rings from both a cross section and a living core from the *Juglans boliviana* collection. These samples were selected based on the mean inter-series correlation at different stages of TRW chronology development (Table 1). The signature of atmospheric radiocarbon from tree-ring cellulose will be referred to as the fraction of modern carbon (F^{14} C). These F^{14} C values can be compared against the global atmospheric radiocarbon curves, which have been divided in latitudinal zones with 3 curves for the Northern Hemisphere (NH) and 2 curves for the Southern Hemisphere (SH), as compiled by Hua et al., (2013, 2021). These curves reflect the high-precision record of atmospheric 14 C variability that spans from \sim 1950 to present, characterized by the nuclear mid 20th century bombing spike in the NH, that rapidly decreased after the ban treaty in 1963 (Hua et al., 2013).

Key years that fall before and after the "bomb-spike" on the ¹⁴C calibration curves were cut from both samples using a #24 scalpel (Table 2). After each year was separated from the sample, it was finely

Table 1

Cofecha mean correlation statistics during chronology development for living, dead, and combined datasets for the final TRW chronology. Note that some calendar dates changed in the development of the chronology and were adjusted based on F¹⁴C measurements for JBX03B and JB013D (see Table 2 and Fig. 2). The first iteration CRN1 represents a dataset with 3 living (last ring assigned to year 2017) and 3 dead trees (last ring assigned to year 2015). CRN2 is composed by 7 living trees and 4 dead trees (last ring re-assigned to 2017). CRN3 represents the final chronology composed by 16 individual living trees and 4 individual cross-sections from dead trees after using dendrochronological proceedings based on assessing the common TRW signal and F¹⁴C results.

		CRN1	CRN2	CRN 3	
Living Trees	Time span	1873–2017	1865–2017	1814–2017	
	No. trees	3	7	16	
	Min-Max corr	0.28-0.57	0.32-0.55	0.31 - 0.58	
	Mean corr	0.43	0.43	0.42	
Dead Trees	Time span	1855-2015	1862-2017	1815-2017	
	No. trees	3	4	4	
	Min-Max corr	0.48-0.68	0.43-0.57	0.38-0.71	
	Mean corr	0.58	0.48	0.53	
Living + Dead	Time span	1855-2017	1865-2017	5-2017 1814-2017	
	No. trees	6	11	20	
	No. radii	10	23	45	
	Max corr	0.24-0.59	0.33-0.6	0.30-0.64	
	Mean corr	0.47	0.47	0.46	

chopped into thinner fibers and weighed (no more than 50 mg of wood) prior to cellulose extraction in individual funnels from our extraction system (Andreu-Hayles et al., 2019). Radiocarbon reference materials were prepared for each extraction run which included fossil wood material AVR-07-PAL-37 (¹⁴C-free), subfossil wood FIRI-H, and post-bomb FIRI-J (barley mash).

Wood samples were exposed to alpha-cellulose extraction protocols using the equipment and proceedings of Andreu-Hayles et al. (2019). During the cellulose extraction process, the wood material is immersed in a series of heated and timed chlorination (NaClO $_2$) and alkaline

(NaOH) treatments to remove components like lignin and hemicellulose in the wood. Due to the carbon-containing buffer used in the chlorination process (acetic acid), we expanded the Andreu-Hayles et al. (2019) protocol to include an acid (1 N HCL 10%) to remove remaining extractive carbon from the cellulose material (methods described in Santos et al., 2020). The mean extraction yield of cellulose-wood for these samples is 42%, meaning that for 100 mg of wood, we may obtain 42 mg of cellulose.

The samples and select standards were processed for cellulose extractions at LDEO and shipped to KCCAMS/UC Irvine for further processing and high precision ¹⁴C measurements in 3 successive batches as the TRW chronology improved in sample size (Table 1). In total 11 cellulose samples from the cross-section JBX03B (Batch#1–3) and 8 cellulose samples from the core JB013D (Batch #3) were measured (Table 2). Following protocols described in Santos et al. (2020), ¹⁴C analysis was conducted using a compact Accelerator Mass Spectrometry (AMS) system (Beverly et al., 2010) which employs online isotope-fractionation analysis and background correction based on the processed fossil wood AVR-07-PAL-37 (Santos et al., 2020). *Juglans boliviana* F¹⁴C results are reported in comparison to the SH ¹⁴C calibration curves Zone 1–2, and 3 for atmospheric ¹⁴C (Hua et al., 2021, 2013).

2.5. Wood anatomical analyses

To supplement conventional visual processing of the ring boundaries in the wood samples we used a WSL sliding microtome to slice a thin lath of wood from the same core and cross-section samples that were analyzed for F^{14} C. The samples were carefully dyed using traditional quantitative wood anatomy (QWA) proceedings described in von Arx et al. (2016) and transferred to a glass slide to view under a compound light microscope. High-resolution images of the rings were taken using an AmScope 12MP Color CMOS Digital Eyepiece Microscope.

Table 2 Tree-ring dates (Schulman and 14 C) and corresponding Radiocarbon metadata for the JBX03B (section) and JB013D (core) for 3 batches of measurements. The monthly adjusted calendar dates for the F^{14} C are based on the SH Zone 1–2 radiocarbon values provided by Hua et al. (2021). In particular, the January 15 and mean October-May F^{14} C values from the Zone 1–2 curve are shown for comparison to the tree-rings (full seasonwood) values. The sample ID # recorded at the KCCAMS/UCI facility for all sample measurements is also included.

	Dendrochronolog	gical calendar dates (SH Zone 1–2 F ¹⁴ C curve values (Hua et al., 2021)			F ¹⁴ C values for <i>Juglans boliviana</i>			
Sample ID	CRN Batch #	Initial calendar year	Corrected calendar year	¹⁴ C monthly adjustment	F ¹⁴ C mean January 15	F ¹⁴ C mean Oct-May	F ¹⁴ C (whole tree ring)	$\pm\sigma$	UCIAMS#
JBX03B		(t)	(t+2)						
	CRN1,	1958	1960	1961.0417	1.2013	1.1970	1.1932	0.0018	251164
	Batch#1	1962	1964	1965.0417	1.6599	1.6435	1.6228	0.0026	251165
		1963	1965	1966.0417	1.6356	1.6388	1.6299	0.0025	251166
		1967	1969	1970.0417	1.5209	1.5283	1.5077	0.0025	251167
	_	1971	1973	1974.0417	1.4201	1.4231	1.4281	0.0026	251168
	CRN2,	1961		1962.0417	1.2113	1.2062	1.2063	0.0016	256179
	Batch#2	1962		1963.0417	1.2693	1.2770	1.2695	0.0017	256180
		1970		1971.0417	1.5048	1.5077	1.5053	0.0020	256181
	_	1971		1972.0417	1.4893	1.4944	1.4857	0.0020	256182
			(t-1)						
	CRN2,	1956	1955	1956.0417	1.0081	1.0051	1.0109	0.0019	261954
	Batch#3	1957	1956	1957.0417	1.0269	1.0232	1.0350	0.0019	261955
			>						
JB013D			(t-3)						
	CRN2,	1955	1952	1953.0417	0.9743	0.9742	0.9879	0.0018	261956
	Batch#3	1956	1953	1954.0417	0.9746	0.9748	0.9726	0.0018	261957
		1960	1957	1958.0417	1.0745	1.0664	1.0487	0.0020	261958
		1961	1958	1959.0417	1.1287	1.1232	1.0987	0.0023	261959
		1962	1959	1960.0417	1.1963	1.1786	1.1727	0.0022	261960
		1963	1960	1961.0417	1.2013	1.1970	1.1845	0.0021	261961
		1969	1966	1967.0417	1.6223	1.6181	1.5986	0.0032	261962
		1970	1967	1968.0417	1.5710	1.5765	1.5740	0.0030	261963

2.6. Mean TRW chronologies

Once the final calendar dates were assigned following visual crossdating based on common TRW patterns among trees, as well as wood anatomy and radiocarbon analysis, each timeseries was detrended using a signal-free age-dependent spline and converged within 7 iterations (Melvin and Briffa, 2008). Conservative detrending methods such as rigid (100, 200-year) splines, horizontal mean, and negative exponential, were also explored to evaluate difference in the resulting standard chronologies, but ultimately the signal-free method of detrending was selected to preserve low-mid frequency information, enhance the common growth signal, and minimize noise due to the uneven growth morphology and age of tree samples (Melvin and Briffa, 2008). The TRW index was calculated using ratios and combined using a robust bi-weight mean to generate the standard chronology (Cook, 1990). The individual standard timeseries were prewhitened using an autoregressive model and were combined to produce the residual chronology (RES) using a robust biweight mean (Cook, 1990).

The mean correlation between the timeseries was calculated both between (r) and within (r.wt) tree samples within the chronology. The Expressed Population Signal (EPS), which measures the predictive power of an n number of samples (Wigley et al., 1984), was also used to determine the number of samples required to produce a robust TRW chronology based on a common, coherent signal. The arbitrary cut-off of 0.85 EPS is used in dendrochronology as an acceptable threshold to indicate that the series composing a chronology shared a considerable amount of variance. We used Pettitt's changepoint detection methods (Pettitt, 1979) to identify a significant shift in low frequency of the mean TRW between 1868 and 2017 (EPS > 0.85) and Sen's Slope calculation (Sen, 1968) to estimate the magnitude of the trend in TRW in the period after the breakpoint. The statistical significance of this trend was evaluated using the non-parametric Mann-Kendall test. All statistical analyses were tested using the trend package in R.

To investigate a potential link between negative TRW outliers and El Niño events, we plotted the years of extreme Niño3.4 SST anomalies (1.5–+2.0 °C) identified by Webb and Magi (2022) in the Ensemble Oceanic Niño Index (ENS-ONI) which combines over 30 reanalysis and reconstruction datasets for the Niño3.4 region (1850–2021). The authors defined 20 'Super' and 'Strong' El Niño events as ENS-ONI values that exceeded 1.5 °C between October through March. The onset year of 17 El Niño events were compared here to the Schulman dated residual chronology for the calibration period (1850–2017).

2.7. Climate sensitivity of Juglans boliviana from MNP

After confirming the annual nature of the Juglans boliviana tree rings, the TRW chronology was finalized and compared to monthly maximum (Tmax), minimum (Tmin), and mean (Tavg) temperatures, and precipitation from the Climate Research Unit reanalysis product 0.5 x 0.0.5° grid resolution (CRU 4.06; Harris et al., 2020). Tmax data was used herein because (1) it has been reported recently to have a greater net impact on tropical tree growth (Sullivan et al., 2020; Zuidema et al., 2022) than minimum (Tmin) and average temperatures (Tavg); (2) correlation analysis between TRW and Tmin did not produce significant results; (3) partial correlations between Tavg and TRW were similar but weaker and less significant than Tmax particularly on a seasonal scale. Analysis with the CRU 4.06 precipitation gridded dataset (Harris et al., 2020) was also conducted though correlations were not significant. In contrast, significant results between TRW and precipitation were obtained using the high-resolution (0.05 × 0.05°) precipitation dataset CHIRPS (Funk et al., 2015), which combines multiple remote sensing products, satellite, and meteorological information. Due to the time span of the CHIRPS product, all climate analyses were conducted for the 1981-2018 period.

To investigate the relationship between year-to-year climate variability and tree growth, the residual TRW chronology was compared

with the residuals from a linear regression applied to the climate data. Comparing the residuals from the datasets minimizes potential bias related to trend and allows for a more accurate assessment of correlation in the high frequency domain.

Bootstrapped Pearson (simple) correlations between the TRW chronologies and monthly (CRU) Tmax and (CHIRPS) precipitation data were calculated from July of the previous year to June of the current year for the period of 1981–2018. This period was chosen for maximum overlap with the CHIRPS product. Due to the significant results with monthly Tmax and CHIRPS, partial correlations were also calculated using averages from 1 to 6-months of climate data to analyze the TRW-climate relationship on a seasonal scale. Partial correlations are used to determine the significance of a simple correlation between TRW and a climate variable (Tmax for example) while considering (and removing) covariance between Tmax and Precipitation (Rodriguez-Caton et al., 2021). All seasonal and monthly correlation analyses were performed using the R-package treeclim (Meko et al., 2011; Zang and Biondi, 2015).

Spatial analysis was next performed to assess the extent of climate signal at a broader scale using correlations between the standard (STD) TRW chronology, mean CRU Tmax (May-August), and mean CHIRPS (May-October) for the period of 1981–2017.

3. Results

3.1. Tree-ring chronology development and radiocarbon results

Table 1 shows the results of statistical analysis of the *Juglans boliviana* TRW chronology as the dataset evolved and the initial assigned dates were corrected. The first chronology (CRN1) is based on 3 living trees dated to 2017 and 3 cross-sections dated to 2015 (with at least 2 radii per tree) that share a common growth signal with a meaninterseries correlation of r=0.47. Cross-section JBX03B, with the ring next to the bark dated as 2015 (t, Schulman date), was selected for independent radiocarbon analysis due to its clear tree-ring boundaries and highest correlation among the TRW samples comprising CRN1.

As seen in Fig. 2A, Batch #1 of radiocarbon measurements shows that the tree rings were in fact annually resolved (i.e., a single ring was produced per growth year) since the F¹⁴C reproduced the shape of the bomb-pulse, but the calendar dates were offset by 2 years forward in time (t+2). For the tree-ring $F^{14}C$ values to match the same calendar years of the SH Zone 1–2 and Zone 3 $\mathrm{F}^{14}\mathrm{C}$ calibration curves, there were two possibilities. First, this individual sample could have 2 false rings between 1972 and 2015. This option was discarded due to the welldefined tree rings observed. A second possibility was that the year of the last ring when the tree died was in fact 2017 instead of 2015. This option seemed more likely, considering the preliminary date of 2015 was assigned to the last ring in the cross-section samples based on the assumption that logging occurred 2 years prior, which could be incorrect (i.e. trees could have felled any time between 2015 and 2018 based on communication with local community), and the correlations in Cofecha between the TRW of the dead and living samples were reasonable (Table 1). This highlights the potential unreliability of exclusively using Cofecha as a tool for establishing calendar dates when the master TRW chronology is formed by an equal number of samples from different subsets, as demonstrated in CRN1 with 3 living and 3 'dead' trees (Table 1).

CRN2 in Table 1 describes the adjusted chronology with the cross-sections (including JBX03B) now ending in 2017, and the addition of 5 individual tree samples (4 living and 1 dead). Although the correlations are lower for the cross-sections, the correlation among the living samples (r=0.43) and among all the samples (r=0.47) remained the same. In CRN2, JBX03B continued to hold the highest correlation with the master chronology among the cross-sections (r=0.57). Based on CRN2 new calendar dating, a second batch (Batch #2) of radiocarbon measurements was made using additional tree rings from JBX03B. The tree-ring 14 C values (CRN2 t) align perfectly with the adjusted calendar

R.C. Oelkers et al. Dendrochronologia 79 (2023) 126090

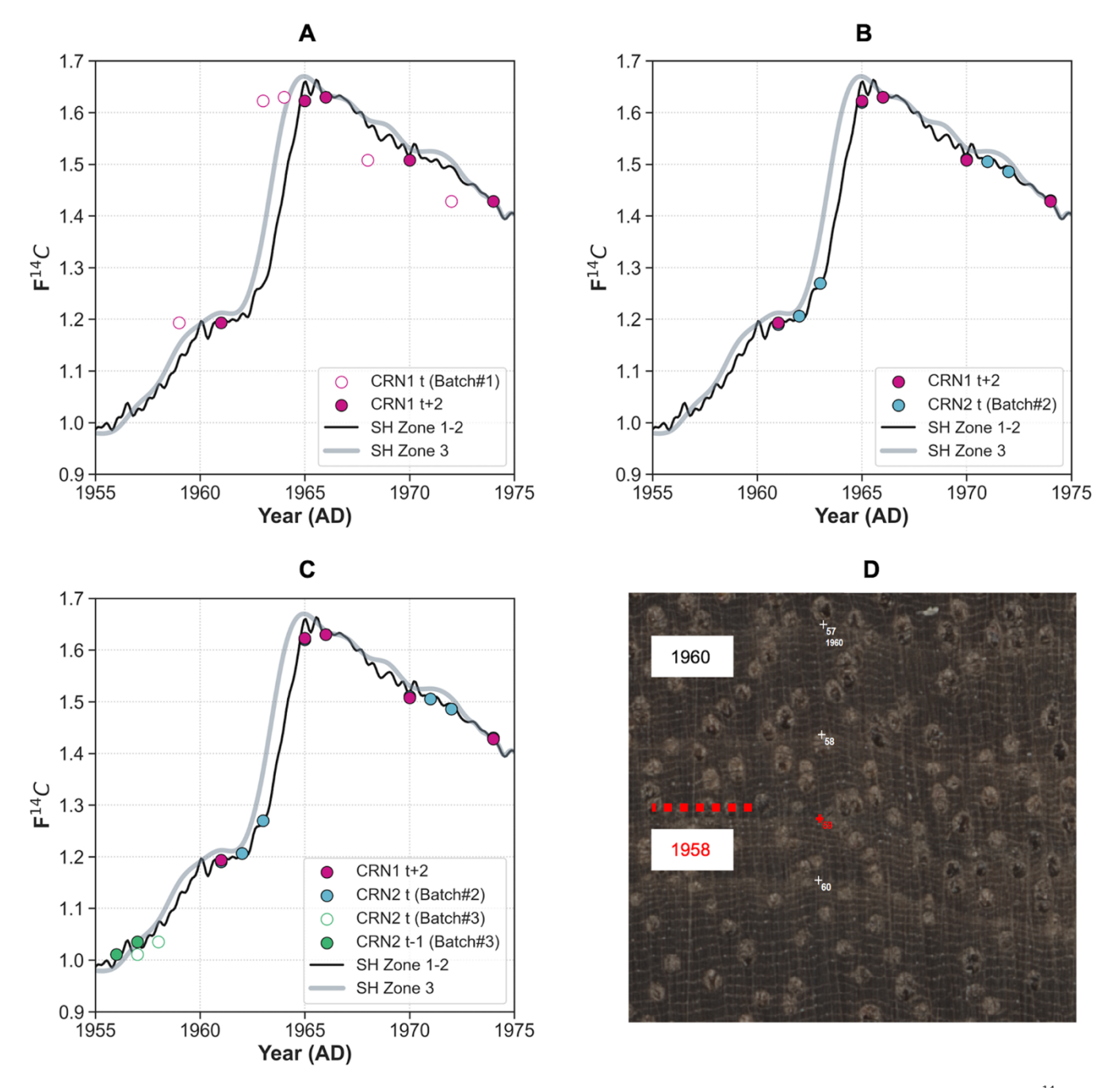


Fig. 2. (A, B, C) Radiocarbon results for cross-section JBX03B plotted with the SH Zone 1–2 and Zone 3 curves (**Hua et al.**, 2021). Open circles represent $F^{14}C$ values and initial calendar dates (t) for the tree-ring samples that were offset in comparison to the SH ^{14}C calibration curves, while filled circles depict adjusted tree-ring dates that reasonably match the SH Zone 1–2 curve. (A) The first run of $F^{14}C$ measurements (Batch#1) for JBX03B (dated to 2015) plotted using the dendro-chronological dates in CRN1 (t, pink open circles) and the same tree-ring $F^{14}C$ values (t + 2) moved 2 years forward in time (pink filled circles). Note that after the adjustment of the 2-year offset the tree-ring $F^{14}C$ fit well with the SH ^{14}C curve Zone 1–2 (pink filled circles, CRN1 t + 2). (B) The second round of ^{14}C measurements (Batch#2, filled blue circles) with calendar dates based on CRN2 (i.e., last ring now 2017 for the sample JBX03B) aligned nicely with the SH Zone 1–2 ^{14}C curve. (C) The last batch of ^{14}C measurements (Batch#3) measured two additional tree rings 1956 and 1957 based on calendar dating in CRN2 and showed a 1-year offset from the curve for those two values. (D) Image from the ring boundary of the Schulman year 1958 (dashed line) that was thought to be a false ring and thus was not included in the samples composing CRN2. However, the Batch#3 $F^{14}C$ results (C) suggested that this ring 1958 is a real, locally absent boundary.

dates (CRN1 t+2) from tree rings measured in Batch #1 (Fig. 2B). The best match of the tree-ring $F^{14}C$ values was found during the uptrend of the ^{14}C bomb-pulse of the SH Zone 1–2 curve (Hua et al., 2021).

To extend the dataset back in time, we evaluated whether the year 1959 contained a false ring and for that purpose, two additional rings from the section JBX03B were sent in Batch#3 of ¹⁴C measurements. Fig. 2C shows that these rings assigned to the years 1956 and 1957 (t, Schulman dates) were offset by 1 year back in time in relation to the SH

Zone $1-2^{14}$ C curves (CRN2 t-1). An image from the program CooRecorder in Fig. 2D shows the suspected false ring in 1959 (t, Schulman dates) that was not included in the CRN2. The ring boundary for this year, 1958, appears irregular across most samples in CRN2 and therefore it was not measured initially. However, when this ring is considered a true ring, the tree-ring F^{14} C values (CRN2 t-1) would align with the SH Zone $1-2^{14}$ C values (Hua et al., 2021).

Some rings of the living core JB013D, selected for its high correlation

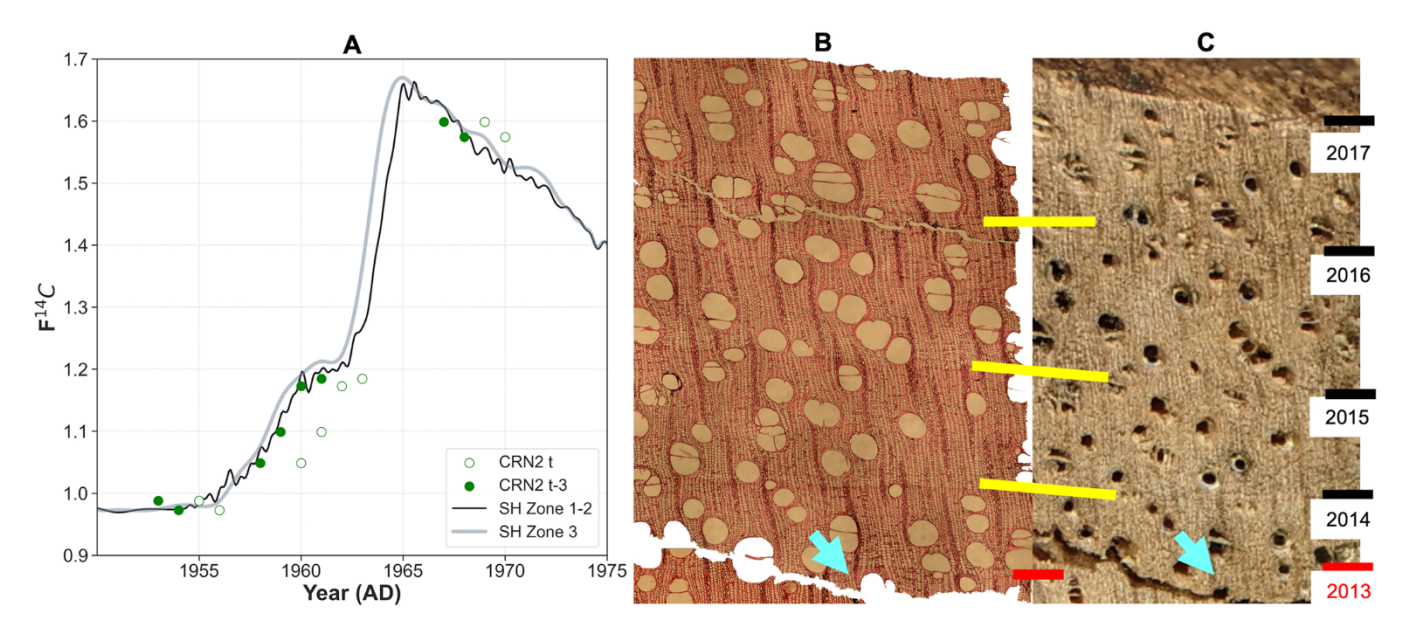


Fig. 3. (A) Radiocarbon measurements for core sample JB013D plotted against the SH Zone 1–2 and Zone 3 ¹⁴C curves (Hua et al., 2021). The dates based on CRN2 (values with open circles) suggest the rings are annual but offset by three years. (B, C) Comparison of anatomical and microscope images of Core 13D rings (years 2017 through part of 2013). Black lines represent rings that were observed originally. The red line (2013) and blue arrows indicate the latewood boundary that was not recognized originally using the microscope, yet clearly visible in the anatomical cut. The light coloration of the sapwood for this core and the thin latewood boundaries of this species highlights the value of using anatomical methods to improve visualization.

with the mean chronology CRN2 (Table 1), were also cut and measured for ¹⁴C measurements in Batch#3. Fig. 3A shows that these *Juglans* trees produced annual rings (t) because the number of rings that were counted on the wood sample appear to follow the same shape and sequential order on the plot. In other words, the symmetry of the ¹⁴C bomb-pulse curve was preserved, but the calendar dates were offset 3 years backwards in time (t-3, open circles). To investigate the sample for potential unmarked rings, anatomical cuts (Fig. 3B) were compared to images under a stereoscope (Fig. 3 C). While the sapwood in JB013D was quite light in appearance making it difficult to identify ring boundaries with the naked eye under a stereomicroscope, the anatomical images allowed for the visualization of the thin latewood boundaries. This is the example of the ring assigned to the year 2013, which was unmarked during the initial tree-ring measurements (Fig. 3B,C). Upon review based on

anatomical cuts, 3 additional tree-ring boundaries were identified between 1986 and 2000. These adjustments in the TRW chronology allowed for 2 additional radii of tree 13 to be crossdated and added into the final chronology CRN3 (Table 1). More details of the mean *Juglans boliviana TRW* chronology can be found in Section 3.3.

Table 2 summarizes the F¹⁴C results for selected rings of the cross-section sample JBX03B (Fig. 2) and living tree JB013D (Fig. 3) samples. The initial and corrected (Schulman) dendrochronological calendar dates are indicated for each version of the chronologies (CRN1, CRN2, and CRN3). The F¹⁴C data from the Hua et al. (2021) SH Zone 1–2 curve is provided on monthly timescales and Table 2 shows the year, monthly adjustment, and ¹⁴C values for January 15 and the average from October-May. These periods were chosen as an approximation of the middle and full extent of the growing season for the Santa Rosa site

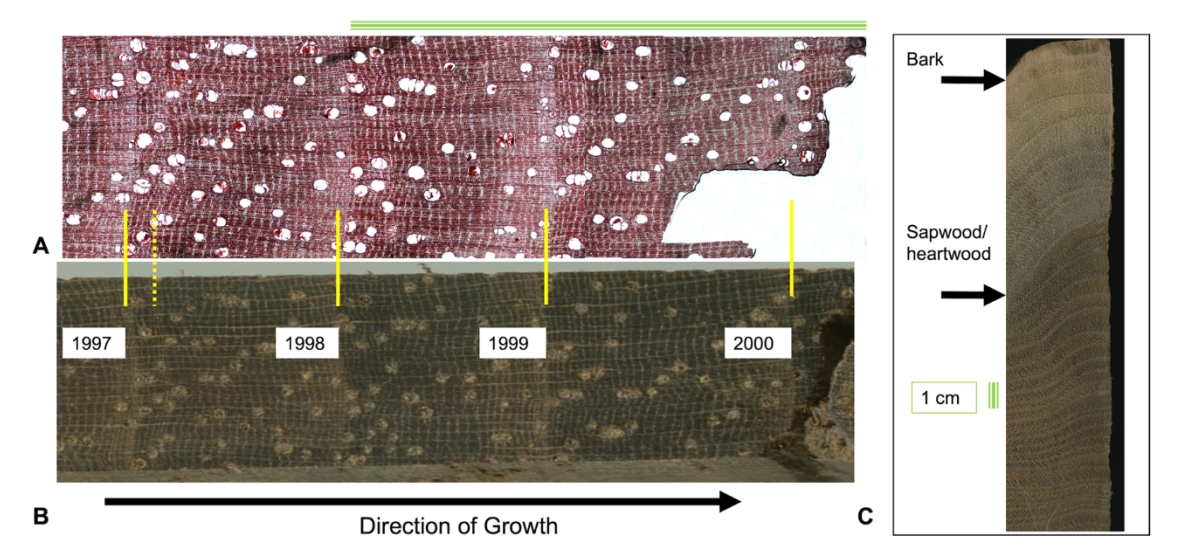


Fig. 4. (A) Microscopic image of JBX03B anatomical cut. (B) Scanned image of the same sample for the Schulman-assigned dates of 1997–2000. Solid yellow lines indicate the end of the ring (latewood boundary), while the dashed line signifies a false ring. (C) Vertical view of the heartwood/sapwood transition for this *Juglans* species as depicted in the sample radii. The faint lightwood in the recently developed rings is quite different than the dark sapwood where ring boundaries are more visible. A green bar representing 1 cm is included for scale (A, C).

(see Section 2.1). The tree ring $F^{14}C$ values align closely to both the January 15 and averaged October-May (i.e. estimated growing season) $F^{14}C$ curve values (Table 2), affirming the corrected calendar dates.

The monthly adjusted decimal of 0.0417, corresponding to the month of January (centered on January 15) in the 14 C curves, was applied to the year the tree stopped growing (Schulman t+1) for visualization purposes in the plot (Fig. 3 C,4 A). For example, the Schulman date 1960 in JBX03B represents the year the tree started growing, and the month of January occurs in the following calendar year (1961), the 14 C adjustment date is 1961.0417.

3.2. Wood anatomical analyses

When working with dark tropical hardwoods trees like Juglans, wood anatomy can be an essential additional tool for robust chronology building. Here we used anatomical cuts to improve the visual identification of 'true' tree rings (Fig. 3B) and to better understand the cellular structure of Juglans boliviana ring boundaries. Like other species of this genus, Juglans boliviana has a diffuse porous wood anatomy characterized by rings with large vessels in the earlywood and terminal parenchyma that define the latewood boundary (Figs. 3B,4A). The axial parenchyma is organized as thin bands which increase in frequency towards the end of the ring as the cell-wall thickness of fiber cells diminishes (Fig. 4A). The increase in the frequency of axial parenchyma without the clear narrow terminal parenchyma cells is indicative of a false ring boundary as seen in the 1997/98 tree ring (Fig. 4A.B). Although it is easier to identify the tree-ring boundaries in the large cross-section sample (Fig. 4C) than in the 5 mm core scan (Fig. 3C), the presence of irregular (pinching) radial patterns in the cross section (Fig. 4C) challenged visual and statistical crossdating among radii. There is a clear heartwood/sapwood transition boundary observed in this cross-section sample that is apparent in most samples for this species as well (Fig. 4C).

A few *Juglans* core samples exhibited dissimilar ring counts (either false rings or locally absent boundaries) and structure along the circumference of the tree. In particular, the sapwood in some of the core samples made the visualization of the thin latewood boundaries difficult and led to dating issues during early iterations of the chronology (Fig. 3B,C). Overall, the enhanced visualization of the tree-rings in

JBX03B and JB013D using anatomical cuts allowed for an improved identification of the tree-ring boundaries and facilitated crossdating and the generation of the final chronology (CRN3, Table 1).

3.3. The Juglans boliviana TRW chronology

Fig. 5 shows the final chronology (CRN3, Table 1) generated for the *Juglans boliviana* site near Santa Rosa, Bolivia. From a total of 29 individual trees (71 radii) initially sampled and sanded, 20 trees (45 radii from 16 cores and 4 cross-sections) were successfully crossdated and individually measured (Fig. 5A) to produce a standard mean chronology spanning from 1814 to 2017 (Fig. 5B). A few trees below 50 cm in diameter could not be crossdated due to young age (< 30 years). The mean age of the samples that reached pith was 115 years old, though some trees were over 200 years in age. The mean correlation among all tree samples (r) and within individual trees (*r.wt*) was 0.46 and 0.541, respectively. This chronology satisfied the 0.85 EPS criterion until 1868 when the sample size (*n*) decreased from 20 to 10 individuals.

The quality of the crossdating is also seen in Fig. 5A, with individual TRW series sharing common variability, particularly for years of high growth. For clarity, the living cores and cross-section samples are colored separately. There is a clear upward trend in growth observed in recent decades which is visible both within the physical wood samples and the detrended TRW timeseries (Fig. 5A). Results of Pettitt's changepoint detection (Fig. 5B) identified 1979 as a breakpoint in standard growth trends (p = 0.006). The median slope between 1979 and 2017 estimated by the Sen slope method and Mann-Kendall test indicated the positive trend was significant (p = 0.002). Although the sample size is low there is clear agreement among trees during years of low growth as well (Fig. 5A,C). When compared to El Niño years, it is interesting to note negative TRW outliers in 1878-79 and 1889-90, which follow the 1877-78 and 1888-89 ('Super') El Niño events that had occurred in the prior growing season, while in the recent period the 1972-73, 1982-83, 1997-98 tree rings were narrow during the same growth-year (t = 0) that El Niño events were recorded (Fig. 5C). Except for the 2009-2010 ring, years of poor growth are observed either during the onset or after the demise (t+1) of extreme ENSO years.

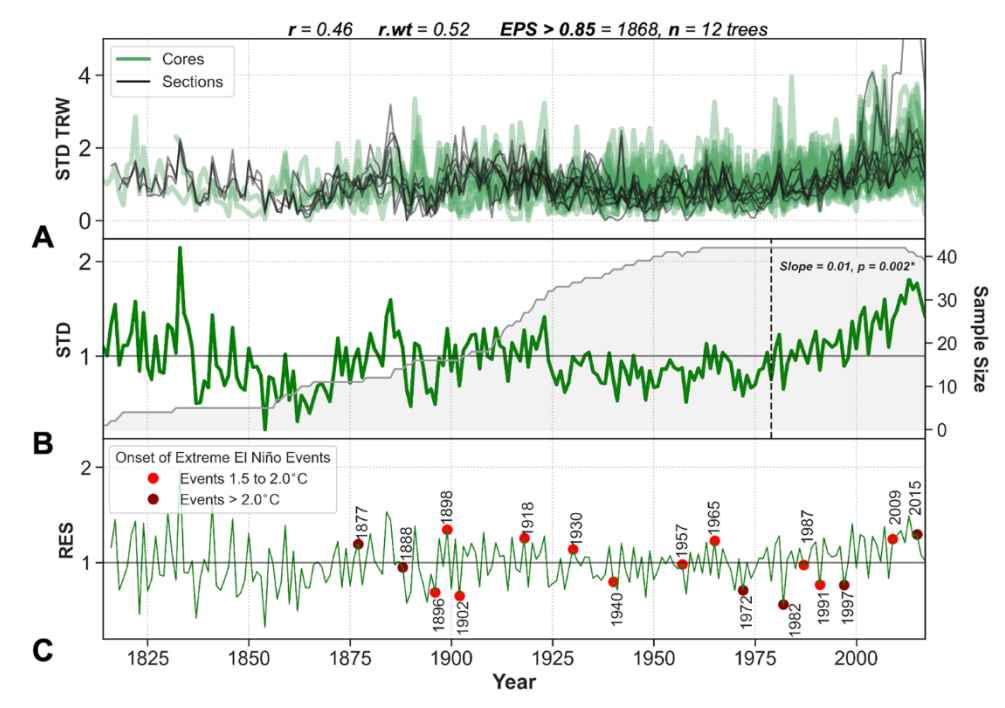


Fig. 5. (A) TRW timeseries from cores (green) and cross-sections (black) of Juglans boliviana detrended using a non-increasing age-dependent spline in SIGFREE (1814-2017). TRW is plotted based on Schulman convention (e.g. dates are based on the calendar year the tree began growing). Chronology statistics such as the mean Pearson correlation among all trees (r) and between radii within a tree (r.wt) are indicated for the entire period. Mean EPS surpassed 0.85 in the year 1868 when the sample size (gray shading, B) reached a minimum of 12 trees. (B) The final standard TRW chronology shows periods of both high and low frequency fluctuations in tree growth over time. The vertical dotted line in the year 1979 represents the breakpoint in the average growth rate detected with Pettitt's changepoint detection test. Sen's slope and Mann-Kendall trend tests verified that the positive trend in TRW between 1979 and 2017 was significant. (C) An increase of TRW in recent years is also present in the residual chronology. Red dots represent the onset of extreme El Niño events as defined by the ENS-ONI (index derived from the Nino3.4 SST region; Webb and Magi, 2022).

3.4. Analyses of growth variability and sensitivity to climate

To investigate the influence of climate on radial growth, we compared the standardized and residual TRW to monthly climate data between 1983 and 2018 from previous July to current year June (Fig. 6). STD TRW variability was negatively correlated with Tmax, particularly during prior-year May and July (r = -0.44, p < 0.05, and r = -0.49, p < 0.05 respectively). Partial correlations with temperature (i.e., after removing the influence of precipitation) remained significant for May and July indicating that this relationship is robust (Fig. 6A). Simple (Tmax as the primary variable) and partial (Tmax as the secondary variable) correlations calculated for two, three, four, five, and six-month seasons showed the negative relationship with maximum temperature remained significant on longer timescales (Fig. S1). The highest correlation was found for the 4-month period of May-August Tmax (r = -0.54, p < 0.05), which coincides with the end of austral summer and the start of the dry season before the current year of growth (Fig. 6A, S1B).

A strong (prior year) dry season temperature signal was also observed for correlations with the residual TRW chronology (Fig. 6B). Similar to the standard chronology, RES TRW variability negatively correlated to maximum temperatures for the months of May (r=-0.34, p<0.05), June (r=-0.34, p<0.05), and July (r=-0.58, p<0.05), before the growing season. Additionally, only for the RES TRW chronology, a negative correlation during peak wet season months (December and January) in the current year of growth was found (Fig. 6B, S1B). A current-year summer signal was also observed in

correlations with mean CRU Temperature in the high frequency (Fig. S2), though correlations between Tmax and TRW were more robust than average temperature overall.

Correlations between the standard and residual TRW chronologies and monthly precipitation exhibited similar temporal signals. There was a strong positive relationship between TRW and monthly precipitation (CHIRPS dataset) during the end of the prior-year (austral) summer and beginning of the current-year spring, with the highest and significant correlation coefficients for the months of May (r = 0.60, p < 0.05) and July (r = 0.50, p < 0.05) (Fig. 6C). Partial correlations for the same months remained significant emphasizing the strength of the precipitation signal. The 2-6-month seasonal correlations (Fig. S3), showed that Juglans boliviana was most sensitive (r = 0.60, p < 0.05) to precipitation during the 6-month period of previous May-current October (Fig. 6C, S2). The same analyses between TRW and CRU precipitation (Fig. S4) showed a significant positive correlation to July and negative correlation to November in the previous growing season, but the temporal response was weaker than the results obtained using the higher resolution CHIRPS (precipitation) dataset (Fig. S3).

Spatial correlations between *Juglans boliviana* STD TRW and May-Aug Tmax (1981–2017) were significant and negative (r=-0.40 to -0.50, p<0.05) locally and across much of the Altiplano (Fig. 7A), but positive near the southwestern Amazon basin. The positive May-Oct precipitation signal extends across the greater Madidi Yungas region into Southern Peru (r=0.40-0.60, p<0.05), highlighting the strength of the imprint of a broader 'off-season' precipitation in TRW variability from 1981 to 2017 (Fig. 7B).

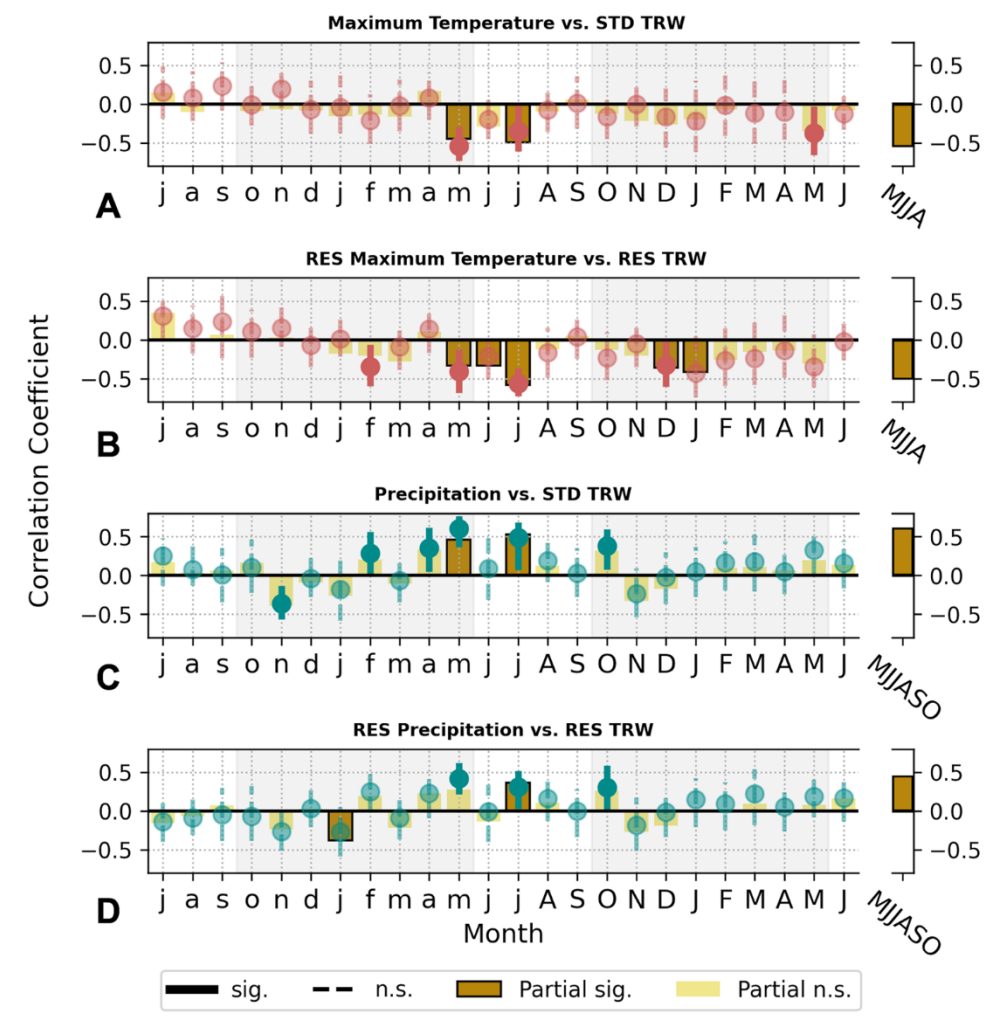


Fig. 6. Climate correlations (1983-2018) with the standard (STD; A,C) and residual (RES; B,D) chronologies for months of the previous (lowercase letters) and current (upper case letters) growth year. Grey shading represents the estimated growing season between October through May. Monthly Pearson correlations against CRU Tmax and CHIRPS precipitation is shown as dashed and solid lines, while partial correlations are depicted as rectangles. For A and B, partial correlations reflect the relationship between TRW and Tmax without the covariance of precipitation (or Tmax for C and D). Significant correlations (p < 0.05) are indicated as solid colors while non-significant are opaque. Overall, there is a negative relationship between Tmax and TRW variability and positive relationship to precipitation variability, particularly during the previous dry season. Simple (primary) and partial (secondary) correlations show Tmax and precipitation during the austral fall and winter months (May, July) hold significance with tree-growth in the high and low frequency domain (A-D).

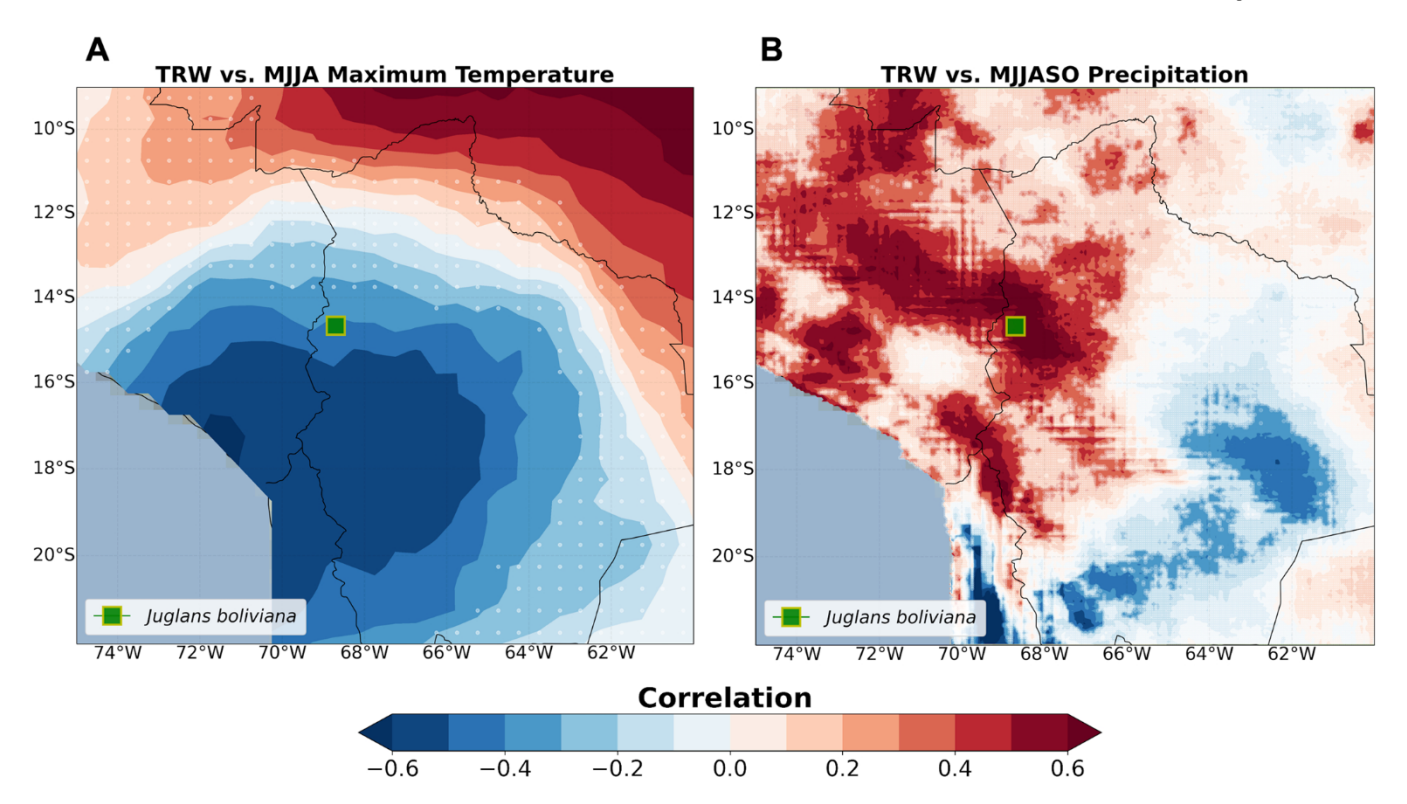


Fig. 7. Spatial correlations of mean TRW vs. Maximum temperatures and precipitation is plotted for the seasons with the strongest correlations for the 1981–2017 period. Regions where TRW significantly correlated to climate are represented by the clear dark colors while non-significant (p > 0.05) areas are masked in white dots. There were significant negative correlations with TMAX (0.5°) across the Altiplano and positive correlations in the Brazilian amazon during the MJJA season (A). During the MJJASO period, TRW variability also showed positive agreement with the higher resolution (0.05°) CHIRPS dataset localized near the site in MNP and across much of the Bolivian-Peruvian Yungas (B). TRW (standard chronology), TMAX, and CHIRPS are plotted for the 1981–2017.

4. Discussion

4.1. A new tree species for dendrochronology

Tropical Andean forests are among the most biodiverse environments in South America, yet there is a limited understanding of tree-age and growth response to climate and anthropogenic change for many of its tree species. Proxy records from tree rings can be critical for understanding historical climate and environmental variability in the tropics, where available instrumental records are short and spatially limited. Here, we have described the first tree-ring width chronology for Juglans boliviana and demonstrated the annual periodicity of its tree rings using an independent approach which combines traditional dendrochronological methods, wood anatomy, and 14C analyses. Cross-sectional samples are very important and even essential in that they allow for visualization of the growth layers along the entire circumference. The heterogeneity of growth rings within a tree can make crossdating and chronology-building quite difficult and the use of computer programs such as Cofecha and Cdendro should be used with caution during initial stages of chronology development when the sample size is low. Although mean correlations among TRW from individual samples appeared reasonable in CRN 1 and 2 (Table 1), independent radiocarbon analysis confirmed that the initial assigned calendar dates were incorrect. F¹⁴C measurements, high individual sample size, and anatomical analysis of the wood were necessary to successfully process the Juglans boliviana tropical wood samples. The final iteration of the TRW chronology has shown these trees can be long-lived (> 200 years), express common variability in the TRW, and are senstive to climate. The results we have presented herein demonstrate the potential to target this species in future dendrochronological work in the tropics.

4.2. The benefits of wood anatomical analyses for tropical dendrochronology

Tree-ring boundaries in dark tropical woods like some tree species from the Juglandaceae family can be difficult to examine using a stereomicroscope alone. The classification of Juglans boliviana wood anatomy has been described previously (Miller, 1976), although further research is needed to explore the growth physiology behind the heterocelullar structure of the radial rings. The miscounted rings in the JB13D sample were better identified with high-quality anatomical images in the sapwood portion that enhanced the clarity of the thin latewood boundaries in the light-colored sapwood (Fig. 3). We thus strongly suggest the use of wood anatomical cuts to aid in visualization of wood anatomical structures, and thus in the identification of tree-ring ring boundaries and false rings and cellular structure in such tropical woods. Microscope cameras like the AmScope 12MP Color CMOS Digital Eyepiece in combination with a compound light microscope are an effective alternative to traditional more expensive systems for taking high quality magnified images of anatomical slides for this purpose. Wood anatomical cuts may be a solution for improved visualization and thus, crossdating in some tropical species (Pacheco-Solana et al., 2023). As seen in the radiocarbon analysis for cross-section JBX03B (Fig. 2), it is possible that dating issues could be prevalent in earlier periods of the TRW chronology (prior to the 1957 ¹⁴C results). However, with the help of an increased sample size and review of anatomical cuts, adjustments can be made to supplement dendrochronological methods and improve the quality of the tropical tree-ring datasets. Innovative approaches to tree-ring visualization such as (green) autofluorescence for example (Godoy-Veiga et al., 2019) may be useful for accurate identification of growth rings in dark tropical wood.

4.3. Tree growth variability and trends

Identifying new species with annual periodicity may provide insights into the rate of growth of forests in understudied regions of the Tropical Andes like the MNP. Most interannual TRW fluctuations for Juglans boliviana appear to correspond to wet and cold(wide TRW) or dry and warm (narrow TRW) years, particularly during the dry season. Additionally, the evidence for a significant monthly and seasonal signal in the residual chronologies (Fig. 6B,D, and Figs. S2,3) indicates that the positive (negative) correlation with dry season precipitation (maximum temperatures) is not just an artifact of trend. The notable, though not unprecedented, recent positive and positive trend in Juglans boliviana growth since 1979 was also observed in Juglans australis from subtropical northwestern Argentina. Villalba et al. (1998) found that wetter Juglans australis sites had higher growth rates in recent decades that coincided with increased precipitation during the dry-wet season transition (April-December). Additionally, Ferrero et al. (2015) successfully developed a May-Oct streamflow reconstruction using Juglans australis samples near the Villalba et al. (1998) sites, further verifying the connection between 'off-season' rainfall and radial growth.

Disentangling the factors contributing to recent growth trends of Juglans boliviana is complex. A recent study in the upper Madeira Basin (near our Juglans boliviana site) found that the highest values for the normalized vegetation index (NDVI) in evergreen forests (which included Madidi National Park and the Amazon) occurred during the transition period between wet-dry (April-May) seasons, with a strong positive NDVI-precipitation relationship at the end of the dry season (Gutierrez-Cori et al., 2021). The authors surmised that forests like Juglans boliviana shift from being light-limited during the peak rainy season (austral summer) to water-limited in the austral fall (peak NDVI) and spring months in the southwestern Amazon basin. Zuidema et al. (2022) found that the higher precipitation variability that occurs during the dry season constrains the climate signal in tropical TRW. In precipitation sensitive trees like the Juglans boliviana reported here, the authors found higher precipitation and lower maximum temperature during the dry season leads to higher growth rates. Our results confirm these previous findings and highlight that water availability during the wet-to-dry and dry-to-wet transitional seasons largely determine Juglans boliviana growth.

Above-ground biomass increased during the late 20th century in humid ecosystems in the Amazon (Baker et al., 2004; Phillips, 1996; Phillips et al., 2016), although trends vary regionally (Brienen et al., 2015; Rahman et al., 2019). In general, increased biomass growth in South America has been linked to increased seasonal water (rather than light) availability (Álvarez-Dávila et al., 2017; Poorter et al., 2017; Zuidema et al., 2022). Species in dense, humid forests, at low elevations, typically compete for light and nutrient resources especially when they are young (Brienen et al., 2022, 2017; Rozendaal et al., 2015). The trees sampled in this study approached or reached canopy level and are at least 50 years old, suggesting that light demand decreased with age and height, and local water supply could be contributing to TRW variability in recent years.

An additional factor that should be considered is the potential for human influence at our sudy site near Santa Rosa. Although the canopy appeared intact during sampling, this recent settlement of native peoples along the Tuichi River occurred during the late 1980's just north of our study site. Therefore, it is possible that local gap dynamics in the forest landscape may have been impacted at some point. The use of signal-free detrending of TRW in one study noted a potential exaggeration of increasing trends in temperature sensitive trees from the northern hemisphere though the authors suggested one cause could be related to the 'even-age' of the tree samples (Pearl et al., 2017); a factor not relevant to the *Juglans boliviana* reported here. Regardless of detrending methods (i.e., conservative methods such as horizontal line, age-dependent, flexible splines), the recent increasing trend shown in the TRW chronology remained apparent and the correlation to climate

variables remained robust when comparing results obtained from standard and residual chronologies. Additionally, the physical appearance of wide rings in the recent period was evident in the wood of most mature trees (> 160 years) like JBX03B (Fig. 4A,C). Further research on stand dynamics and tree physiology (i.e., water-use efficiency) is needed to determine the ecological drivers associated with the observed higher growth rates during the most recent years (Rahman et al., 2019).

Climate analysis in the tropics is challenging due to the poor spatial coverage of climate data in South America in general. The lack of significant results between growth and CRU precipitation in this study (Fig. S3) could be attributed to the lower resolution of the CRU 0.5° grid box that includes meteorological stations far away from the site. Temperature is less variable than precipitation in the greater tropical region; thus, less bias is expected. Although the accuracy of CHIRPS data during the dry season (JJA) is weaker than in the wet season months (Canedo-Rosso et al., 2021), our results appear robust for that period and are in agreement with climate response reported by other tropical *Juglans* species mentioned above.

Although dry-season precipitation in the southwestern Amazon is largely influenced by SSTAs from the tropical north Atlantic and the recycling of moisture within the Amazon basin (Espinoza et al., 2019; Zuidema et al., 2022), negative TRW outlier years observed in the current or subsequent growth year after known El-Niño events suggest that the Juglans boliviana trees could be influenced by summertime precipitation anomalies associated with the Pacific Ocean as well. Austral summer Pacific Ocean signals recorded in tree-ring records has been reported with varying responses of TRW to ENSO-related anomalies depending on the location and altitude of the trees along the central Andes. Studies near the Bolivian Altiplano (Christie et al., 2009; Crispín-DelaCruz et al., 2022; Morales et al., 2012) found that P. tarapacana trees had smaller rings in years with below-average summer (Dec-Feb) rainfall associated with warm ENSO phases in the Niño3.4 tropical Pacific region (El Niño), and extremely wide tree rings during extreme wet years related to cold ENSO events (La niña). In contrast, in eastern Bolivia where El Niño is associated with increased rainfall and flooding, tree rings from a lowland tropical dry site recorded high years of growth (Paredes-Villanueva et al., 2013). However, the strength of precipitation response to ENSO phases on the eastern slope of the Bolivian Cordillera (Jonaitis et al., 2021; Ronchail and Gallaire, 2006) is complex and can vary due to topography or spatiotemporal moisture variability in and out of the Amazon and Altiplano (Garreaud, 2009). Although the sample size could be increased and further analysis is required, the common growth signal of Juglans boliviana observed during periods of known climate extremes is encouraging and provides incentive to target mid-elevation Andes-Amazon transition forests for future dendroclimatological studies. Additional development of well-replicated tropical tree-ring width chronologies will help us to further constrain our understanding of the complex forest hydroclimate dynamics of tropical South America and vicinity.

5. Conclusions

Only a small number of tree species from northern Bolivia have been used for dendrochronological research to date. The confirmation of annual periodicity for *Juglans boliviana* herein represents the introduction of a new tree species suitable for dendrochronological research in the tropics. Traditional dendrochronological methods should be supplemented with independent calendar dating and visualization techniques (e.g., radiocarbon and wood anatomical analyses) to produce reliable datasets for some tropical species growing under humid environments. Implementing these combined methods could also benefit for tropical studies around the world. As for *Juglans* studies from the submontane tropical Andes, a rapid growth increase since the 1979 was observed herein for *Juglans boliviana*, with a significant positive relationship to precipitation variability and negative relationship to maximum temperature variability in the months before peak wet season.

R.C. Oelkers et al. Dendrochronologia 79 (2023) 126090

The longevity of this species shows potential for a new paleoclimate archive in a region with low-quality and short instrumental records. Future chronologies from this species will allow us to better constrain our understanding of tree growth, past climate variability, and the response of forests to anthropogenic change in the Bolivian and Peruvian Yungas.

Funding

This work was supported by the U.S. National Science Foundation (NSF) projects AGS-1702789, OISE-1743738 and AGS-1903687. MEF was partially supported by Agencia Nacional de Promoción Científica y Tecnológica (ANPCyT), PICT-2019-01336 PMO BID (Argentina). G.M.S. thanks U.S. National Science Foundation for support (AGS-1703035 and AGS-1903690).

Declaration of Competing Interest

The authors declare that they have no known competing financial interests or personal relationships that could have appeared to influence the work reported in this paper.

Data Availability

Data will be made available on request.

Acknowledgements

Rose dedicates this paper to the National Herbarium of Bolivia, native community of Santa Rosa, and team members of the Madidi Project, without whom this research would not be possible. We thank Troy Nixon and Jessica Geary for their support in wood sample preparation and Clara Rodriguez-Morata for assistance in cellulose extractions.

Appendix A. Supporting information

Supplementary data associated with this article can be found in the online version at doi:10.1016/j.dendro.2023.126090.

References

- Álvarez-Dávila, E., Cayuela, L., González-Caro, S., Aldana, A.M., Stevenson, P.R., Phillips, O., Cogollo, Á., Peñuela, M.C., Hildebrand, P., von, Jiménez, E., Melo, O., Londoño-Vega, A.C., Mendoza, I., Velásquez, O., Fernández, F., Serna, M., Velázquez-Rua, C., Benítez, D., Rey-Benayas, J.M., 2017. Forest biomass density across large climate gradients in northern South America is related to water availability but not with temperature. PLOS ONE 12, e0171072. https://doi.org/10.1371/journal.pone.0171072.
- Andreu-Hayles, L., Levesque, M., Martin-Benito, D., Huang, W., Harris, R., Oelkers, R., Leland, C., Martin-Fernández, J., Anchukaitis, K.J., Helle, G., 2019. A high yield cellulose extraction system for small whole wood samples and dual measurement of carbon and oxygen stable isotopes. Chem. Geol. 504, 53–65. https://doi.org/ 10.1016/j.chemgeo.2018.09.007.
- Araujo-Murakami, A., Zenteno, Zenteno-Ruiz, F., 2006. Bosques de los Andes orientales de Bolivia y sus especies útiles.
- Baker, J.C.A., Santos, G.M., Gloor, M., Brienen, R.J.W., 2017. Does Cedrela always form annual rings? testing ring periodicity across South America using radiocarbon dating. Trees 31, 1999–2009. https://doi.org/10.1007/s00468-017-1604-9.
- Baker, T.R., Phillips, O.L., Malhi, Y., Almeida, S., Arroyo, L., Di Fiore, A., Erwin, T., Higuchi, N., Killeen, T.J., Laurance, S.G., Laurance, W.F., Lewis, S.L., Monteagudo, A., Neill, D.A., Núñez Vargas, P., Pitman, N.C.A., Silva, J.N.M., Vásquez Martínez, R., 2004. Increasing biomass in Amazonian forest plots. Philos. Trans. R. Soc. Lond. B. Biol. Sci. 359, 353–365. https://doi.org/10.1098/rstb.2003.1422.
- Beverly, R.K., Beaumont, W., Tauz, D., Ormsby, K.M., von Reden, K.F., Santos, G.M., Southon, J.R., 2010. The keck carbon cycle AMS laboratory, university of california, irvine: status report. Radiocarbon 52, 301–309. https://doi.org/10.1017/ S0033822200045343.
- Boninsegna, J.A., Argollo, J., Aravena, J.C., Barichivich, J., Christie, D., Ferrero, M.E., Lara, A., Le Quesne, C., Luckman, B.H., Masiokas, M., Morales, M., Oliveira, J.M., Roig, F., Srur, A., Villalba, R., 2009. Dendroclimatological reconstructions in South

- America: a review. Palaeogeogr. Palaeoclimatol. Palaeoecol. 281, 210–228. https://doi.org/10.1016/j.palaeo.2009.07.020.
- Brienen, R., Helle, G., Pons, T., Boom, A., Gloor, M., Groenendijk, P., Clerici, S., Leng, M., Jones, C., 2022. Paired analysis of tree ring width and carbon isotopes indicates when controls on tropical tree growth change from light to water limitations. Tree Physiol. 42, 1131–1148. https://doi.org/10.1093/treephys/tpab142.
- Brienen, R.J.W., 2005. Tree rings in the tropics: a study on growth and ages in Bolivian rain forest trees. PROMAB, Riberalta, Beni, Bolivia.
- Brienen, R.J.W., Zuidema, P.A., 2006. Lifetime growth patterns and ages of Bolivian rain forest trees obtained by tree ring analysis. J. Ecol. 94, 481–493. https://doi.org/ 10.1111/j.1365-2745.2005.01080.x.
- Brienen, R.J.W., Phillips, O.L., Feldpausch, T.R., Gloor, E., Baker, T.R., Lloyd, J., Lopez-Gonzalez, G., Monteagudo-Mendoza, A., Malhi, Y., Lewis, S.L., Vásquez Martinez, R., Alexiades, M., Álvarez Dávila, E., Alvarez-Loayza, P., Andrade, A., Aragão, L.E.O.C., Araujo-Murakami, A., Arets, E.J.M.M., Arroyo, L., Aymard C, G.A., Bánki, O.S., Baraloto, C., Barroso, J., Bonal, D., Boot, R.G.A., Camargo, J.L.C., Castilho, C.V., Chama, V., Chao, K.J., Chave, J., Comiskey, J.A., Cornejo Valverde, F., da Costa, L., de Oliveira, E.A., Di Fiore, A., Erwin, T.L., Fauset, S., Forsthofer, M., Galbraith, D.R., Grahame, E.S., Groot, N., Hérault, B., Higuchi, N., Honorio Coronado, E.N., Keeling, H., Killeen, T.J., Laurance, W.F., Laurance, S., Licona, J., Magnussen, W.E., Marimon, B.S., Marimon-Junior, B.H., Mendoza, C., Neill, D.A., Nogueira, E.M., Núñez, P., Pallqui Camacho, N.C., Parada, A., Pardo-Molina, G., Peacock, J., Peña-Claros, M., Pickavance, G.C., Pitman, N.C.A., Poorter, L., Prieto, A., Quesada, C.A., Ramírez, F., Ramírez-Angulo, H., Restrepo, Z., Roopsind, A., Rudas, A., Salomão, R. P., Schwarz, M., Silva, N., Silva-Espejo, J.E., Silveira, M., Stropp, J., Talbot, J., ter Steege, H., Teran-Aguilar, J., Terborgh, J., Thomas-Caesar, R., Toledo, M., Torello-Raventos, M., Umetsu, R.K., van der Heijden, G.M.F., van der Hout, P., Guimarães Vieira, I.C., Vieira, S.A., Vilanova, E., Vos, V.A., Zagt, R.J., 2015. Long-term decline of the Amazon carbon sink. Nat. 519, 344-348. https://doi.org/10.1038/ nature14283.
- Brienen, R.J.W., Schöngart, J., Zuidema, P.A., 2016. Tree rings in the tropics: insights into the ecology and climate sensitivity of tropical trees. In: Tropical Tree Physiology: Adaptations and Responses in a Changing Environment. Springer International Publishing, Switzerland, p. 441.
- Brienen, R.J.W., Gloor, E., Clerici, S., Newton, R., Arppe, L., Boom, A., Bottrell, S., Callaghan, M., Heaton, T., Helama, S., Helle, G., Leng, M.J., Mielikäinen, K., Oinonen, M., Timonen, M., 2017. Tree height strongly affects estimates of water-use efficiency responses to climate and CO₂ using isotopes. Nat. Commun. 8, 288. https://doi.org/10.1038/s41467-017-00225-z.
- Canedo-Rosso, C., Hochrainer-Stigler, S., Pflug, G., Condori, B., Berndtsson, R., 2021. Drought impact in the Bolivian Altiplano agriculture associated with the El Niño-Southern Oscillation using satellite imagery data. Nat. Hazards Earth Syst. Sci. 21, 995–1010. https://doi.org/10.5194/nhess-21-995-2021.
- Carlquist, S., 2001. Comparitive Wood Anatomy, second ed. Springer-Verlag, Berlin Heidelberg, New York.
- Christie, D.A., Lara, A., Barichivich, J., Villalba, R., Morales, M.S., Cuq, E., 2009. El Niño-Southern Oscillation signal in the world's highest-elevation tree-ring chronologies from the Altiplano, Central Andes. Palaeogeogr. Palaeoclimatol. Palaeoecol. 281, 309–319. https://doi.org/10.1016/j.palaeo.2007.11.013.
- Cook, E.R., Briffa, K.R., Shiyatov, S., Mazepa, V., 1990. Tree-ring Stand. Growth-Trend Estim. 104–123.
- Crispín-DelaCruz, D.B., Morales, Marianos., Andreu-Hayles, Laia, Christie, DuncanA., Guerra, A., Requena-Rojas, EdilsonJ., 2022. High ENSO sensitivity in tree rings from a northern population of Polylepis tarapacana in the Peruvian Andes. Dendrochronologia 71, 125902. https://doi.org/10.1016/j.dendro.2021.125902.
- De Lucca, M., Zalles, J., 1992. Flora medicinal boliviana. Dicc. Enciclopédico Paz Los Amigos Libro.
- Espinoza, J.C., Ronchail, J., Marengo, J.A., Segura, H., 2019. Contrasting North–South changes in Amazon wet-day and dry-day frequency and related atmospheric features (1981–2017. Clim. Dyn. 52, 5413–5430. https://doi.org/10.1007/s00382-018-4462-2.
- Ferrero, M.E., Villalba, R., De Membiela, M., Ripalta, A., Delgado, S., Paolini, L., 2013. Tree-growth responses across environmental gradients in subtropical Argentinean forests. Plant Ecol. 214, 1321–1334. https://doi.org/10.1007/s11258-013-0254-2.
- Ferrero, M.E., Villalba, R., De Membiela, M., Ferri Hidalgo, L., Luckman, B.H., 2015. Tree-ring based reconstruction of Río Bermejo streamflow in subtropical South America. J. Hydrol. 525, 572–584. https://doi.org/10.1016/j.jhydrol.2015.04.004.
 Fritts, H.C., 1976. Tree Rings and Climate. Academic Press, London.
- Fuentes, A., 2005. Una Introd. a la Veg. De. la región De. Madidi 32.
- Funk, C., Peterson, P., Landsfeld, M., Pedreros, D., Verdin, J., Shukla, S., Husak, G., Rowland, J., Harrison, L., Hoell, A., 2015. The climate hazards infrared precipitation with stations—a new environmental record for monitoring extremes. Sci. Data 2, 1–21.
- Garreaud, R.D., 2009. The Andes climate and weather. Adv. Geosci. 22, 3–11. https://doi.org/10.5194/adgeo-22-3-2009.
- Godoy-Veiga, M., Slotta, F., Alecio, P.C., Ceccantini, G., Buckeridge, M.S., Locosselli, G. M., 2019. Improved tree-ring visualization using autofluorescence. Dendrochronologia 55, 33–42. https://doi.org/10.1016/j.dendro.2019.03.003.
- Gutierrez-Cori, O., Espinoza, J.C., Li, L.Z.X., Wongchuig, S., Arias, P.A., Ronchail, J., Segura, H., 2021. On the hydroclimate-vegetation relationship in the Southwestern Amazon During the 2000–2019 Period. Front. Water 3, 648499. https://doi.org/ 10.3389/frwa.2021.648499.
- Harris, I., Osborn, T.J., Jones, P., Lister, D., 2020. Version 4 of the CRU TS monthly high-resolution gridded multivariate climate dataset. Sci. Data 7, 109. https://doi.org/10.1038/s41597-020-0453-3.

R.C. Oelkers et al. Dendrochronologia 79 (2023) 126090

Herrera-Ramirez, D., Andreu-Hayles, L., del Valle, J.I., Santos, G.M., Gonzalez, P.L.M., 2017. Nonannual tree rings in a climate-sensitive Prioria copaifera chronology in the Atrato River, Colombia. Ecol. Evol. 7, 6334–6345. https://doi.org/10.1002/ ecos. 2905

- Holmes, R.L., 1983. Computer-assisted quality control in tree-ring dating and measurement. Tree-Ring Bull. 43, 69–78.
- Hua, Q., Barbetti, M., Rakowski, A.Z., 2013. Atmospheric radiocarbon for the Period 1950–2010. Radiocarbon 55, 2059–2072. https://doi.org/10.2458/azu_js_rc.
- Hua, Q., Turnbull, J.C., Santos, G.M., Rakowski, A.Z., Ancapichún, S., De Pol-Holz, R., Hammer, S., Lehman, S.J., Levin, I., Miller, J.B., Palmer, J.G., Turney, C.S.M., 2021. Atmos. Radiocarb. PERIOD 1950–2019.
- Humanes-Fuente, V., Ferrero, M.E., Muñoz, A.A., González-Reyes, Á., Requena-Rojas, E. J., Barichivich, J., Inga, J.G., Layme-Huaman, E.T., 2020. Two centuries of hydroclimatic variability reconstructed from tree-ring records over the Amazonian Andes of Peru. J. Geophys. Res. Atmospheres 125. https://doi.org/10.1029/2020.ID032565.
- Inga, J.G., del Valle, J.I., 2017. Log-relative growth: A new dendrochronological approach to study diameter growth in Cedrela odorata and Juglans neotropica, Central Forest, Peru. Dendrochronologia 44, 117–129. https://doi.org/10.1016/j. doi:10.2017/03.000
- Jonaitis, J.A., Perry, L.B., Soulé, P.T., Thaxton, C., Andrade-Flores, M.F., Vargas, T.I., Ticona, L., 2021. Spatiotemporal patterns of ENSO-PRECIPITATION relationships in the tropical Andes of southern Peru and Bolivia. Int. J. Climatol. 41, 4061–4076. https://doi.org/10.1002/joc.7058.
- La Porte, J., 1966. Números cromosómicos y algunas observaciones biológicas sobre tres especies americanas del género Juglans. Darwiniana 14, 156-160.
- López, L., Villalba, R., 2011. Climate influences on the radial growth of centrolobium microchaete, a valuable timber species from the tropical dry forests in bolivia: climate influences on valuable timber tree. Biotropica 43, 41–49. https://doi.org/ 10.1111/j.1744-7429.2010.00653.x.
- López, L., Villalba, R., 2016. An assessment of Schinopsis brasiliensis Engler (Anacardiacea) for dendroclimatological applications in the tropical Cerrado and Chaco forests, Bolivia. Dendrochronologia 40, 85–92. https://doi.org/10.1016/j. dendro.2016.07.002.
- López, L., Villalba, R., Peña-Claros, M., 2012. Determining the annual periodicity of growth rings in seven tree species of a tropical moist forest in Santa Cruz, Bolivia. . Syst. 21, 508. https://doi.org/10.5424/fs/2012213-02966.
- López, L., Villalba, R., Stahle, D., 2022. High-fidelity representation of climate variations by Amburana cearensis tree-ring chronologies across a tropical forest transition in South America. Dendrochronologia 72, 125932. https://doi.org/10.1016/j. dendro.2022.125932.
- Macía, M.J., 2008. Woody plants diversity, floristic composition and land use history in the Amazonian rain forests of Madidi National Park, Bolivia. Biodivers. Conserv. 17, 2671–2690. https://doi.org/10.1007/s10531-008-9348-x.
- Manning, W.E., 1948. The morphology of the flowers of the juglandaceae. III. The staminate flowers. Am. J. Bot 35, 606–621. https://doi.org/10.2307/2438058.
- Manning, W.E., 1960. The Genus Juglans in South America and the West Indies. Brittonia 12, 1. https://doi.org/10.2307/2805331.
- Meko, D.M., Touchan, R., Anchukaitis, K.J., 2011. Seascorr: A MATLAB program for identifying the seasonal climate signal in an annual tree-ring time series. Comput. Geosci. 37, 1234–1241. https://doi.org/10.1016/j.cageo.2011.01.013.
- Melvin, T.M., Briffa, K.R., 2008. A "signal-free" approach to dendroclimatic standardisation. Dendrochronologia 26, 71–86. https://doi.org/10.1016/j. dendro.2007.12.001.
- Miller, R.B., 1976. Wood anatomy and identification of species of juglans. Bot. Gaz. 137, 368–377. https://doi.org/10.1086/336886.
- Morales, M.S., Villalba, R., Grau, H.R., Paolini, L., 2004. Rainfall-controlled tree growth in high-elevation subtropical treelines. Ecology 85, 3080–3089. https://doi.org/ 10.1890/04-0139.
- Morales, M.S., Christie, D.A., Villalba, R., Argollo, J., Pacajes, J., Silva, J.S., Alvarez, C. A., Llancabure, J.C., Soliz Gamboa, C.C., 2012. Precipitation changes in the South American Altiplano since 1300 AD reconstructed by tree-rings. Clim 8, 653–666. https://doi.org/10.5194/cp-8-653-2012.
- Morales, M.S., Cook, E.R., Barichivich, J., Christie, D.A., Villalba, R., LeQuesne, C., Srur, A.M., Ferrero, M.E., González-Reyes, Á., Couvreux, F., Matskovsky, V., Aravena, J.C., Lara, A., Mundo, I.A., Rojas, F., Prieto, M.R., Smerdon, J.E., Bianchi, L.O., Masiokas, M.H., Urrutia-Jalabert, R., Rodriguez-Catón, M., Muñoz, A.A., Rojas-Badilla, M., Alvarez, C., Lopez, L., Luckman, B.H., Lister, D., Harris, I., Jones, P.D., Williams, A. P., Velazquez, G., Aliste, D., Aguilera-Betti, I., Marcotti, E., Flores, F., Muñoz, T., Cuq, E., Boninsegna, J.A., 2020. Six hundred years of South American tree rings reveal an increase in severe hydroclimatic events since mid-20th century. Proc. Natl. Acad. Sci. 117, 16816–16823. https://doi.org/10.1073/pnas.2002411117.
- Mostacedo C, B., Fredericksen, T.S., 1999. Regeneration status of important tropical forest tree species in Bolivia: assessment and recommendations. . Ecol. Manag 124, 263–273. https://doi.org/10.1016/S0378-1127(99)00076-6.
- Pacheco-Solana, A., Oelkers, R., D'Arrigo, R., Santos, G.M., Rodriguez-Caton, M., Tejedor, E., Ferrero, E., Fuentes, A.F., Maldonado, C., Andreu-Hayles, L., 2023. Radiocarbon and wood anatomy as complementary tools for generating tree-ring records in Bolivia. Front. Plant Sci. 14.
- Paniagua-Zambrana, N.Y., Bussmann, R.W., Romero, C., 2020. Juglans boliviana (C. DC.) Dode Juglans neotropica Diels Juglandaceae. In: Paniagua-Zambrana, N.Y., Bussmann, R.W. (Eds.), Ethnobotany of the Andes. Springer International Publishing, Cham, pp. 1–9. https://doi.org/10.1007/978-3-319-77093-2_155-1.
- Paredes-Villanueva, K., Sánchez-Salguero, R., Manzanedo, R.D., Sopepi, R.Q., Palacios, G., Navarro-Cerrillo, R.M., 2013. Growth rate and climatic response of

- machaerium scleroxylon in a dry tropical forest in southeastern Santa Cruz, Bolivia. Tree-Ring Res 69, 63–79. https://doi.org/10.3959/1536-1098-69.2.63.
- Paredes-Villanueva, K., López, L., Brookhouse, M., Cerrillo, R.M.N., 2015. Rainfall and temperature variability in Bolivia derived from the tree-ring width of Amburana cearensis (Fr. Allem.) A.C. Smith. Dendrochronologia 35, 80–86. https://doi.org/ 10.1016/j.dendro.2015.04.003.
- Pettitt, A.N., 1979. A non-parametric approach to the change-point problem. J. R. Stat. Soc. Ser. C. Appl. Stat. 28, 126–135. https://doi.org/10.2307/2346729.
- Phillips, O.L., 1996. Long-term environmental change in tropical forests: increasing tree turnover. Environ. Conserv. 23, 235–248. https://doi.org/10.1017/ S0376892900038856.
- Phillips, O.L., Lewis, S.L., Higuchi, N., Baker, T., 2016. Recent changes in Amazon forest biomass and dynamics. In: Interactions between Biosphere, Atmosphere and Human Land Use in the Amazon Basin. Springer, pp. 191–224.
- Poorter, L., van der Sande, M.T., Arets, E.J.M.M., Ascarrunz, N., Enquist, B.J., Finegan, B., Licona, J.C., Martínez-Ramos, M., Mazzei, L., Meave, J.A., Muñoz, R., Nytch, C.J., de Oliveira, A.A., Pérez-García, E.A., Prado-Junior, J., Rodríguez-Velázques, J., Ruschel, A.R., Salgado-Negret, B., Schiavini, I., Swenson, N.G., Tenorio, E.A., Thompson, J., Toledo, M., Uriarte, M., Hout, P., van der, Zimmerman, J.K., Peña-Claros, M., 2017. Biodiversity and climate determine the functioning of Neotropical forests. Glob. Ecol. Biogeogr. 26, 1423–1434. https://doi. org/10.1111/geb.12668.
- Quesada-Román, A., Ballesteros-Cánovas St., J.A., George, S., Stoffel, M., 2022. Tropical and subtropical dendrochronology: approaches, applications, and prospects. Ecol. Indic. 144, 109506 https://doi.org/10.1016/j.ecolind.2022.109506.
- Rahman, M., Islam, M., Gebrekirstos, A., Bräuning, A., 2019. Trends in tree growth and intrinsic water-use efficiency in the tropics under elevated CO₂ and climate change. Trees 33, 623–640. https://doi.org/10.1007/s00468-019-01836-3.
- Ramírez, F., Kallarackal, J., 2021. The phenology of the endangered Nogal (Juglans neotropica Diels) in Bogota and its conservation implications in the urban forest. Urban Ecosyst. 24, 1327–1342. https://doi.org/10.1007/s11252-021-01117-3.
- Rodriguez-Caton, M., Andreu-Hayles, L., Morales, M.S., Daux, V., Christie, D.A., Coopman, R.E., Alvarez, C., Rao, M.P., Aliste, D., Flores, F., Villalba, R., 2021. Different climate sensitivity for radial growth, but uniform for tree-ring stable isotopes along an aridity gradient in Polylepis tarapacana, the world's highest elevation tree species. Tree Physiology 41 (8), 1353–1371.
- Ronchail, J., Gallaire, R., 2006. ENSO and rainfall along the Zongo valley (Bolivia) from the Altiplano to the Amazon basin. Int. J. Clim. 26, 1223–1236. https://doi.org/ 10.1002/joc.1296.
- Rozendaal, D.M.A., During, H.J., Sterck, F.J., Asscheman, D., Wiegeraad, J., Zuidema, P. A., 2015. Long-term growth patterns of juvenile trees from a Bolivian tropical moist forest: shifting investments in diameter growth and height growth. J. Trop. Ecol. 31, 519–529. https://doi.org/10.1017/S0266467415000401.
- Santos, G.M., Granato-Souza, D., Barbosa, A.C., Oelkers, R., Andreu-Hayles, L., 2020. Radiocarbon analysis confirms annual periodicity in Cedrela odorata tree rings from the equatorial Amazon. Quat. Geochronol. 58, 101079 https://doi.org/10.1016/j. quageo.2020.101079.
- Schöngart, J., Bräuning, A., Barbosa, A.C.M.C., Lisi, C.S., de Oliveira, J.M., 2017.
 Dendroecological Studies in the Neotropics: History, Status and Future Challenges.
 In: Amoroso, M.M., Daniels, L.D., Baker, P.J., Camarero, J.J. (Eds.), Dendroecology:
 Tree-Ring Analyses Applied to Ecological Studies, Ecological Studies. Springer
 International Publishing, Cham, pp. 35–73. https://doi.org/10.1007/978-3-319-61669-8 3.
- Schulman, E., 1956. Dendroclimatic Changes in Semiarid America. University of Arizona Press, Tucson, p. 142.
- Sen, P.K., 1968. Estimates of the regression coefficient based on Kendall's Tau. J. Am. Stat. Assoc. 63, 1379–1389. https://doi.org/10.1080/01621459.1968.10480934.
- Soliz-Gamboa, C.G., Rozendaal, D.M.A., Ceccantini, G., Angyalossy, V., van der Borg, K., Zuidema, P.A., 2011. Evaluating the annual nature of juvenile rings in Bolivian tropical rainforest trees. Trees 25, 17–27. https://doi.org/10.1007/s00468-010-0468-z.
- Stone, D.E., Oh, S.-H., Tripp, E.A., G, L.E.R., Manos, P.S., 2009. Natural history, distribution, phylogenetic relationships, and conservation of Central American black walnuts (Juglans sect. Rhysocaryon)1. J. Torre Bot. Soc. 136, 1–25. https://doi.org/ 10.3159/08-RA-036R.1.
- Sullivan, M.J., Lewis, S.L., Affum-Baffoe, K., Castilho, C., Costa, F., Sanchez, A.C., Ewango, C.E., Hubau, W., Marimon, B., Monteagudo-Mendoza, A., 2020. Long-term thermal sensitivity of Earth's tropical forests. Science 368, 869–874.
- Vanegas, E.T., Rojas, I.C.R., 2018. Estado del arte, propagación y conservación de Juglans neotropica Diels., en zonas andinas. Madera Bosques 24. https://doi.org/ 10.21829/myb.2018.2411560.
- Villalba, R., Boninsegna, J.A., Holmes, R.L., 1985. Cedrela angustifolia and Juglans australis: two new tropical species useful in dendrochronology.
- Villalba, R., Grau, H.R., Boninsegna, J.A., Jacoby, G.C., Ripalta, A., 1998. Tree-ring evidence for long-term precipitation changes in subtropical South America. Int. J. Climatol. 18, 1463–1478. https://doi.org/10.1002/(SICI)1097-0088(19981115)18: 13<1463::AID-JOC324>3.0.CO;2-A.
- von Arx, G., Crivellaro, A., Prendin, A.L., Čufar, K., Carrer, M., 2016. Quantitative wood anatomy—practical guidelines. Front. Plant Sci. 7.
- Webb, E.J., Magi, B.I., 2022. The Ensemble Oceanic Niño Index. Int. J. Clim. 42, 5321–5341. https://doi.org/10.1002/joc.7535.
- Wigley, T.M.L., Briffa, K.R., Jones, P.D., 1984. On the average value of correlated time series, with applications in dendroclimatology and hydrometeorology. J. Appl. Meteorol. Climatol. 23, 201–213. https://doi.org/10.1175/1520-0450(1984) 023<0201:0TAVOC>2.0.CO;2.

- Worbes, M., 1999. Annual growth rings, rainfall-dependent growth and long-term growth patterns of tropical trees from the Caparo Forest Reserve in Venezuela. J. Ecol. 87, 391–403. https://doi.org/10.1046/j.1365-2745.1999.00361.x.
- Yamaguchi, D.K., 1991. A simple method for cross-dating increment cores from living trees. Can. J. . Res. 21, 414–416. https://doi.org/10.1139/x91-053.
- Zang, C., Biondi, F., 2015. treeclim: an R package for the numerical calibration of proxyclimate relationships. Ecography 38, 431–436. https://doi.org/10.1111/ ecog.01335.
- Zuidema, P.A., Babst, F., Groenendijk, P., Trouet, V., Abiyu, A., Acuña-Soto, R., Adenesky-Filho, E., Alfaro-Sánchez, R., Aragão, J.R.V., Assis-Pereira, G., Bai, X., Barbosa, A.C., Battipaglia, G., Beeckman, H., Botosso, P.C., Bradley, T., Bräuning, A., Brienen, R., Buckley, B.M., Camarero, J.J., Carvalho, A., Ceccantin, G., Centeno-Erguera, L.R., Cerano-Paredes, J., Chávez-Durán, Á.A., Cintra, B.B.L., Cleaveland, M. K., Couralet, C., D'Arrigo, R., del Valle, J.I., Dünisch, O., Enquist, B.J., Esemann-

Quadros, K., Eshetu, Z., Fan, Z.-X., Ferrero, M.E., Fichtler, E., Fontana, C., Francisco, K.S., Gebrekirstos, A., Gloor, E., Granato-Souza, D., Haneca, K., Harley, G. L., Heinrich, I., Helle, G., Inga, J.G., Islam, M., Jiang, Y., Kaib, M., Khamisi, Z.H., Koprowski, M., Krujit, B., Layme, E., Leemans, R., Leffler, A.J., Lisi, C.S., Loader, N. J., Locosselli, G.M., Lopez, L., López-Hernández, M.I., Lousada, J.L.P.C., Mendivelso, H.A., Mokria, M., Montóia, V.R., Moors, E., Nabais, C., Ngoma, J., Nogueira Júnior, F., de, C., Oliveira, J.M., Olmedo, G.M., Pagotto, M.A., Panthi, S., Pérez-De-Lis, G., Pucha-Cofrep, D., Pumijumnong, N., Rahman, M., Ramirez, J.A., Requena-Rojas, E.J., Ribeiro, A., de, S., Robertson, I., Roig, F.A., Rubio-Camacho, E. A., Sass-Klaassen, U., Schöngart, J., Sheppard, P.R., Slotta, F., Speer, J.H., Therrell, M.D., Toirambe, B., Tomazello-Filho, M., Torbenson, M.C.A., Touchan, R., Venegas-González, A., Villalba, R., Villanueva-Diaz, J., Vinya, R., Vlam, M., Wils, T., Zhou, Z.-K., 2022. Tropical tree growth driven by dry-season climate variability. Nat. Geosci. 15, 269–276. https://doi.org/10.1038/s41561-022-00911-8.